Article

Incorporating Landscape Dynamics in Small-Scale Hydropower Site Location Using a GIS and Spatial Analysis Tool: The Case of Bohol, Central Philippines

Imelida Torrefranca [1,2,*], Roland Emerito Otadoy [3,4] and Alejandro Tongco [1]

1 Graduate School of Engineering, University of San Carlos, Talamban, Cebu City 6000, Philippines; aftongco@usc.edu.ph
2 Department of Agricultural and Biosystems Engineering, Bohol Island State University, Bilar 6319, Philippines
3 Theoretical, Computational Sciences and Engineering Group, Department of Physics, University of San Carlos, Talamban, Cebu City 6000, Philippines; rsotadoy@usc.edu.ph
4 Center for Geoinformatics and Environmental Solutions, University of San Carlos, Talamban, Cebu City 6000, Philippines
* Correspondence: imetorrefranca@gmail.com or imelida.torrefranca@bisu.edu.ph

Abstract: Hydropower depends on the elevation head and water flow of a river. However, other factors must be considered, such as the risk associated with surface processes and environmental factors. The study aims to analyze a landscape's dynamics and locate potential sites for small-scale hydropower systems (<10 MW) using a geographic information system, the curve number method, and the TopoToolbox with a digital elevation model and available spatial datasets. Across Bohol Island in the central Philippines, the study found 94 potential sites with hydraulic heads ranging from 20–62.4 m, river discharges between 0.02 to 9.71 m^3/s, and a total hydropower capacity of 13.595 MW. The river profile analysis classified the sites to five levels of risk to geo-hazards, with three-fourths of the sites being at 'high' to 'very high' risk levels while more than 50% of the total power can be generated in 'low' risk areas. Land-use and population constraints reduced the sites to 25 and the hydropower capacity by 60%. Although limited to the table assessment phase of hydropower development, the study showed the potential of small-scale hydropower systems in the study area, their spatial distribution, and the risk associated with each site. The study results provided data-limited resource managers' and energy planners' insights in targeting potential locations and minimizing field investigation costs and time.

Keywords: landscape dynamics; small-scale hydropower; GIS; TopoToolbox; CN method; geomorphic index

1. Introduction

The increasing environmental issues associated with fossil-based energy production, depleting sources, and increasing energy demand have led to intensifying use, development, and exploration of alternative renewable energy resources [1–3]. For tropical islands with rich natural resources that suffer from nature's vicissitudes adversely affecting energy supply, searching for more energy sources becomes urgent [4].

Hydropower is one of the world's renewable energy resources. A high-resolution assessment of global hydropower potential by Hoes et al. [2] revealed that about a third of the annual energy requirement can be provided by hydropower but existing hydropower plants produced only 3% of the yearly energy needs. One of the notable features of hydropower sources, especially the small-scale systems (SHP), is the lesser greenhouse gas emission [1,5,6]. The run-of-river small hydropower has become more cost-effective than mini-grids powered by diesel gen-sets due to falling energy costs [7]. IRENA [7] commended the micro-hydro power systems as a better option for household lighting

than the commonly used solar PV in areas where the resource is available for a cluster of households. The SHPs supported rural development in many developing countries in Asia and Africa [8]. Such systems helped improve remote areas' productivity and contributed directly to the development of women by powering small agro-industries usually performed by hand and almost entirely by women [8].

Recent studies compare the impacts of SHP and large-scale hydropower (LHP) systems. Different indicators were evaluated and the demarcations between scales also differ which led to contrasting results. For example, in Duero Basin, Spain, Mayor et al. [9] found that the cumulative impacts of the deployment of many SHPs outweighed the impacts of a few LHP upon evaluating indicators under three categories of energy, water, and environment. An installed capacity of 10 MW demarcates the SHP from the LHP was used in the study [9]. In contrast, Zhang et al. [6] analysis in Tibet, China, found that SHPs have reduced externalities compared to LHPs, considering greenhouse gas emission translated into CO_2 equivalent: SHPs and LHPs produced an average of 5.1 and 29.2 g CO_2-e per kWh, respectively. Reservoir impoundment and occupation were the critical components of the total externality of LHP, the study emphasized. One implication of their study was that a higher power density can decrease externality, which favor the SHP systems. In this study of Zhang et al. [6], an installed capacity of 50 MW was used to differentiate the two hydropower scales. A unified system of evaluation particularly on the indicators to be assessed and the scale to delineate between SHP and LSP may be put forward to resolve opposing results.

The hydropower potential in the Philippines is high [7,10], with untapped resources amounting to 13,097 MW. In 2018, the hydropower share was only 9.4% of the total generation mix of 99,765 GWh [11]. The ADB [10] associated the low hydropower utilization in the country to 'global isolation and the lack of financial and technical capacity'.

Hydropower produces electrical energy from moving water converted through mechanical turbines. The amount of power generated is directly proportional to the head and the flow. In particular, the small-scale hydropower systems depend on the available head and sufficient water flow in the river [12]. Along river channels, locating suitable sites for hydropower plants is a bit challenging [13,14]. A range of factors including hydraulic head, catchment area, flow characteristics, and sensitive environmental issues such as biodiversity and land use pattern must be critically considered in finding potential sites. In response, several studies have developed methods and approaches for identifying potential hydropower sites.

In the last few decades, geographic information systems coupled with hydrologic models were the primary tools employed to identify potential sites for hydropower development. In Pakistan's data-scarce Kunhar River Basin, Moiz et al. [13] developed a geographic information system-based decision-support system for decision-makers evaluating potential hydropower schemes. The system optimized the site selection process for run-of-river small hydropower plants using topographic and hydrologic factors. Bayazit et al. [15] applied GIS-based hydrological modeling with a topographical and meteorological dataset to analyze the hydropower potential of the Bilecik Regional Sakarya Basin, Turkey. Thin et al. [11] integrated GIS and the Soil and Water Assessment Tool (SWAT) and developed a GIS-based tool using Python to locate potential hydropower in Myanmar's Myitnge River Basin. Similarly, Sekac et al. [15] adopted GIS and remote sensing technology to identify potential hydropower sites in the Busu River Catchment in Papua New Guinea. Sammartano et al. [16] also employed GIS and SWAT model to determine the optimal potential run-of-river sites in Taw at Umberleigh Catchment of South West England. Their study assessed the small hydropower projects' environmental and economic feasibility and conducted a multi-objective analysis to highlight profitable schemes. In the Philippines, a geographic information system and a hydrologic model were employed to identify potential hydropower sites in two separate river basins in Mindanao, Philippines [17,18]. Both studies explored possible renewable energy resources to address the perennial energy crisis through hydropower development. A comprehensive method was developed in

the study of [19] to ensure cost-effectiveness and high-performance hydropower projects in the Fomanat Plain of Gilan, Iran. In Estonia, Tamm and Tamm [20], proposed a virtual hydropower assessment method in identifying other potential locations in all large rivers where hydropower plants already existed and found several suitable sites for mini- and micro-hydro types.

The initial assessment for potential hydropower sites centered on topographic and hydrologic factors. Initial investigations commonly assessed larger rivers or major watersheds in an area, neglecting the potential of smaller catchments. The conventional approach may have overlooked the potential of small systems in these areas, which may be beneficial to small clusters of users.

Another observation is that existing studies gave less attention to geomorphic features in a landscape related to surface processes and, thereby, to geomorphic hazards. Geomorphic hazards [21] 'are natural processes until they intersect with human activities and settlements'. These hazards are either natural or anthropogenic to some degree and usually happen along or adjacent to river channels. Hydropower facilities are sited along or adjacent to river channels, and the stability of hillslopes and channels is critical to the sustainability of the engineering structures [22,23]. Although these factors are critically evaluated in the subsequent phase of system development, it is valuable to have such information earlier to have a priority list of potential sites.

Geomorphologists analyzed river profiles to extract information on landscape evolution and the processes that shape the topography of landscapes [24], linking climate, tectonic and surface processes across a landscape [25]. The geomorphic index such as the river steepness index [22,24] and the presence of knickpoints [26] are proxies of natural surface processes. As Boulton [26] noted, steeper channels and regions undergoing higher erosion and uplift rates, can be recognized with river profile analysis as indicated by the high river steepness index. Similarly, the study of Castillo et al. [27] in western Mexico rivers found high river steepness index values that suggests high rock uplift and erosion rates that control the topography of river basins. The river steepness index is a commonly used index to analyze river profiles to infer erosion rates, bedrock erodibility and highlight areas of tectonic activity [24]. Knickpoints, on the other hand, are sharp changes in the channel slope [28] that reflects conditions and processes associated with erosion, lithological changes, and uplift rates. Boulton [26] noticed that knickpoints formed in response to changes in uplift rates are found in areas where river steepness index is high. Chen et al. [29] found steep rivers with many tectonic knickpoints in the eastern flank of the central range of the Taiwanese island where the mountains are under rapid collisional processes. Low river steepness index values indicate low uplift rates [29].

The study presents a rapid method of assessing the dynamics of a landscape for identifying potential sites for small-scale hydropower projects (<10 MW). Specifically, the study aims to (a) examine the topography from a digital elevation model to locate potential sites along river channels, (b) estimate surface runoff using the CN method, (c) compute the hydropower capacity of each site, (d) investigate the geometric indices associated with geo-hazards and (e) analyze the existing land-use and population data. The study is limited to the initial stage of hydropower development. It is applied to an island landscape where natural disasters like typhoons and earthquakes challenge energy supply and accessibility. Results are presented as maps showing the landscape's hydropower potential, the spatial distribution of potential sites, and the risk levels associated with each site. The study results are expected to benefit local resource managers, decision-makers, and energy planners faced with limited data for analysis, in identifying potential sites, targeting directly potential areas and minimizing field investigation costs and time.

2. Methods

Figure 1 shows the workflow of the analysis, and a detailed discussion follows. Data processing started with a topographic analysis that defined the streamlines and determined the required elevation head. Next, the hydrologic analysis provided an estimate of the

flow rate passing through each identified potential site. The two primary factors, elevation head, and flow are inputs to compute the potential hydropower at each site. Then, the river profile analysis determined the geomorphic indices of surface processes associated with channel stability. Lastly, we considered population and land use in the constraint analysis.
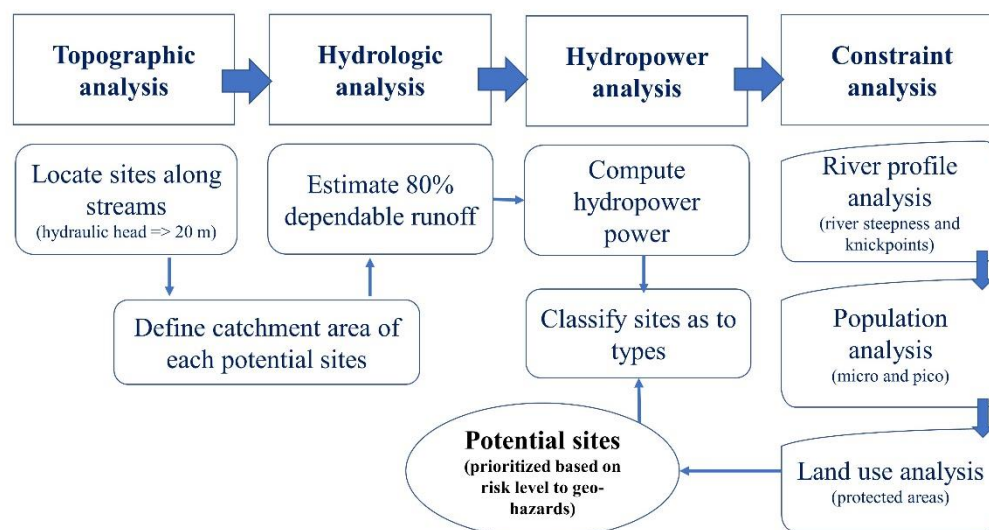
Figure 1. General workflow of the identification of potential small-scale hydropower sites.

2.1. Datasets

The study gathered the required input datasets from several sources as given in Table 1 and processed them following Figure 1 (a detailed process flow is given in Appendix A Figure A1). Table 1 presents a list of all the datasets used, their sources, and data format.

Table 1. List of datasets, their sources, format, derived layer, and type used in the study.

Data	Source	Data Format	Derived Layer	Type
5-m IfSAR DEM	DA-BAR project [1]	TIFF	Stream Elevation head	Raster
Hydrologic Soil Group (HSG) Data	ORNL DAAC [2]	TIFF	Curve number	Raster
Precipitation	WorldClim [3]	TIFF	Average monthly precipitation	Raster
Protected area	WDPA [4] DENR 7 [5]	Shapefile		Vector
Local flow and rainfall data	Loboc Hydroelectric Plant (LHEP)	Spreadsheet		
2015 CENSUS (barangay population)	PSA [6]	Spreadsheet	Population density	Vector/Raster
Annual global land cover change maps	Copernicus [7]	TIFF	Land cover/land use	Raster
Barangay boundary	PhilGIS [8]	Shapefile	Population density map	Raster

[1] Small scale irrigation project (SSIP) funded by the Department of Agriculture—Bureau of Agricultural Research (DA-BAR), Philippines. [2] Global hydrologic soil groups (HYSOGs250m) for curve number-based runoff modeling—https://daac.ornl.gov/ (accessed on 25 August 2021) —Oak Ridge National Laboratory Distributed Active Archive Center (ORNL DAAC), NASA Earth Data. [3] WorldClim is a database of high spatial resolution global weather and climate data. https://www.worldclim.org/data/worldclim21.html (accessed on 1 September 2021). [4] World database on protected areas (WDPA) www.protectedplanet.net (accessed on 5 September 2021). [5] Philippine Department of Environment and Natural Resources (DENR) 7. [6] Philippine Statistics Authority https://psa.gov.ph/ (accessed on 8 June 2021). [7] Copernicus Land Monitoring Service https://land.copernicus.eu/ (accessed on 10 August 2021). [8] Philippine GIS data clearinghouse http://philgis.org/ (accessed on 10 June 2021).

Digital elevation model (DEM). The digital elevation data is critical in the study since this is the primary data where the rest of the analysis depends. In a GIS platform, we preprocessed a DEM and used it to delineate watersheds, determine drainage lines, and compute elevation differences. The DEM is also the primary input to a terrain analysis tool for river profile analysis.

Global datasets. Due to the limited availability of local soil and landcover data, we used freely available global datasets on monthly precipitation, hydrologic soil group, and landcover. The global hydrologic soil group (HYSOGs250m) for curve number-based runoff modeling [30] represents a globally consistent, gridded dataset of hydrologic soil group with a geographical resolution of 1/480 decimal degrees, equivalent to a projected resolution of approximately 250-m. The soil texture classes and depth to bedrock information provided by the Food and Agriculture Organization soilGrids250m system are the bases for classifying the HSG. The Copernicus Global Land Service [31] global landcover dataset provides spatial information on different types (classes) of the Earth's surface physical coverage, e.g., forests, grasslands, croplands, lakes, and wetlands. We used the annual dataset, a moderate resolution landcover map targeting landcover detection and its changes.

Climate data. The WorldClimv2.1 climate data for 1970–2000 [32] provide monthly total precipitation. This dataset was downloaded and used in the runoff determination using the CN method.

Local flow and rainfall data. Flow and rainfall data are available from the monitoring activity of a hydropower plant. The study used the flow and the rainfall data from local rain gauges to describe the area's hydrology but not estimate the surface runoff.

Population data. The study used the 2015 census of the Philippine Statistics Authority (PSA) population data at the barangay (village) level. The data were linked to a barangay shapefile to create a raster surface describing the spatial variability of population density across the study area.

2.2. Topographic Analysis

The topographic analysis examined a DEM (see Appendix A Figure A2) to locate potential sites in the study area. The process is outlined in a model builder created in ArcGIS, as shown in Figure 2. The model builder used a DEM to create the flow direction and flow accumulation rasters. The flow direction raster shows the flow direction from each cell to its steepest downslope neighbor, while the flow accumulation raster shows the accumulated flow into each cell. From the flow accumulation raster, the cells with values of at least 10,000 (equivalent to 100 ha upslope area) were selected using the SetNull tool, creating a new flow accumulation raster. The new flow accumulation raster was used as an input to create the stream raster. Then, the elevation values following the stream raster were extracted and analyzed. The Focal Analysis Tool with a rectangular neighborhood of the same height and width at 100 m was used to determine the maximum elevation in a 100-m channel segment. The channel length was adopted from the study by Sammartano et al. [16]. The elevation head is the difference between the maximum elevation and the local elevation rasters, stored as the elevation head raster. From the elevation head raster, raster values equal to or greater than 20 m ($\geq$20 m) were selected using the Set Null tool. The 20 m minimum head which was adopted from previous studies in the study area [33] and in Uganda [34]. The minimum head value anticipated the low flows from the small catchment and from the upper part of the watersheds which can still produce power at 20 m head or higher. These selected raster values were converted into point vector.

The conversion resulted in clusters of points, as shown in Figure 3, where points were found to assemble around channel segments. For each cluster, a point was selected based on the elevation head value and the location of the point. For instance, in a cluster found at the convergence of two different stream orders, high consideration is given to a point along the higher-order stream because the flow is expected to be higher in high-order stream than in

low-order stream. The study manually picked a point to represent each cluster. A distance of at least 500 m between selected points from each cluster was maintained by using the distance tool. The 500-m minimum site spacing is commonly adopted (ex. [13,33,35]) to allow river ecosystem rejuvenation. These selected points were the potential sites for small-scale hydropower.
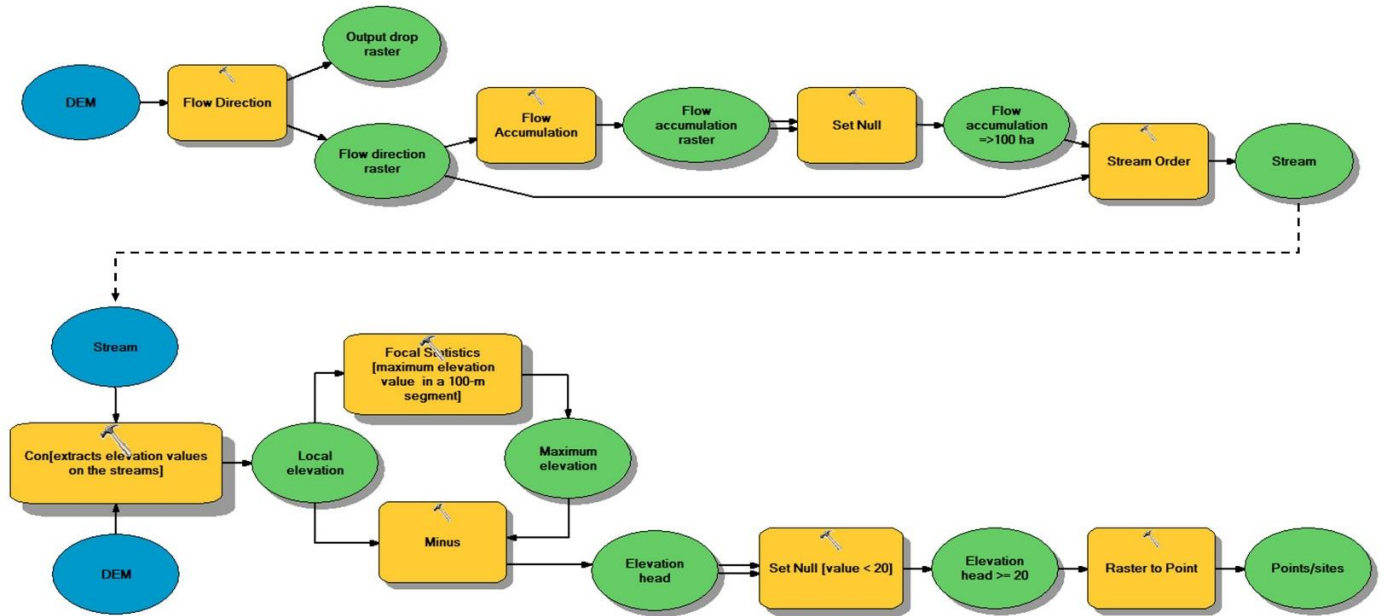
Figure 2. A model builder created for locating points with a minimum elevation head of 20 m along river channels. The yellow-colored rectangle with the hammer sign indicates the toolset used in the analysis. The blue-colored oval shape indicates the input data while the green-colored indicates the output.
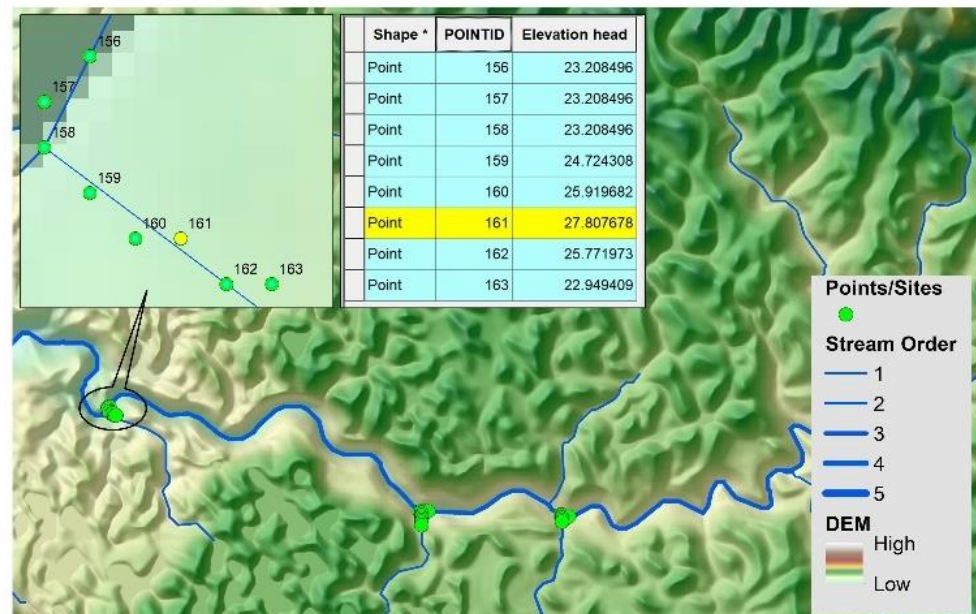
Figure 3. Points clustering on river segments. The selection of a representative point considers the location and the elevation value.

2.3. Runoff Estimation Using CN Method

Several studies used the USDA-CRS curve number (CN) method for estimating surface runoff [36–38]. Due to its simplicity, the study adopted the CN method to estimate direct

surface runoff at each identified potential site. The CN method requires only precipitation values and a single parameter called CN to estimate the direct surface runoff using the equation:

$$q = (R - I_a)^2 / (R - I_a + S),$$ (1)

where q is the accumulated runoff or rainfall excess (mm), R is the rainfall depth (mm), I_a is the initial abstraction (mm), and S is the potential maximum retention (mm). USDA-CRS [39] estimated I_a as 20% of S based on its extensive database. Meanwhile, S is expressed in terms of CN as:

$$S = (25400/CN) - 254.$$ (2)

With this, (1) is written as:

$$q = (R - 0.2\,S)^2 / (R + 0.8\,S).$$ (3)

Equation (2) derived the S raster and then (3) computed the monthly surface runoff q with the corresponding R monthly precipitation data.

The CN factor was estimated based on landcover information and hydrologic soil group described in Tables 2 and 3, respectively. The study used the HYSOGs250m [30], a gridded dataset of hydrologic soil groups (HSGs) with approximately 250-m projected resolution. Ross et al. [30] derived the HSG classification from the soil textural classes and depth to bedrock of the FAO soilGrids250m system to support USDA-based CN runoff modeling. Based on the dataset, the study area has two standard soils, HSG C and HSG D, corresponding to moderately high and high runoff potential, respectively.

Table 2. Description and Curve Numbers of different land uses and hydrologic conditions under different hydrologic soil groups (TR-55).

Land Use (USDA-SCS)	Cover Description		Curve Number for Hydrologic Soil Group			
	Cover Type and Hydrologic Condition	% Impervious Areas	A	B	C	D
Agricultural	Row-crops-straight rows + crop residue cover good condition [1]		64	75	82	85
Commercial	Urban Districts: Commercial and Business	85	89	92	94	95
Forest	Woods [2]—Good Condition		30	55	70	77
Grass/pasture	Pasture, Grassland, or Range [3]—Good Condition		39	61	74	80
High density residential	Residential districts by average lot size: 1/8 acre or less	65	77	85	90	92
Industrial	Urban district: Industrial	72	81	88	91	93
Low density residential	Residential districts by average lot size: $\frac{1}{2}$-acre lot	25	54	70	80	85
Open spaces	Open Space (lawns, parks, golf courses, cemeteries, etc.) [4] Fair Condition (grass cover 50% to 70%)		49	69	79	84
Parking and paved areas	Impervious areas: Paved parking lots, roofs, driveways, etc. (excluding right-of-way)	100	98	98	98	98
Water/wetlands		0	0	0	0	0

Notes: [1] Hydraulic condition is based on combination factors that affect infiltration and runoff, including (a) density and canopy of vegetative areas, (b) amount of year-round cover, (c) amount of grass or close-seeded legumes, (d) percent of residue on the land surface (good ≥ 20%), and © degree of surface roughness. [2] Good: Woods are protected from grazing, and litter and brush adequately cover the soil. [3] Good: >75% ground cover and lightly or only occasionally grazed. [4] 'CN's shown are equivalent to those of pasture. Composite CNs may be computed for other combinations of open space cover types. Source: https://engineering.purdue.edu/mapserve/LTHIA7/documentation/scs.htm (accessed on 5 September 2021).

Table 3. The Global hydrologic soil group and its description.

Pixel Values	Description
1	HSG-A: low runoff potential (>90% sand and <10% clay)
2	HSG-B: moderately low runoff potential (50–90% sand and 10–20% clay)
3	HSG-C: moderately high runoff potential (<50% sand and 20–40% clay)
4	HSG-D: high runoff potential (<50% sand and >40% clay)
11	HSG-A/D: high runoff potential unless drained (>90% sand and <10% clay)
12	HSG-B/D: high runoff potential unless drained (50–90% sand and 10–20% clay)
13	HSG-C/D: high runoff potential unless drained (<50% sand and 20–40% clay)
14	HSG-D/D: high runoff potential unless drained (<50% sand and >40% clay)

Source: Ross, C.W., L. Prihodko, J. Anchang, S. Kumar, W. Ji, and N.P. Hanan. 2018. HYSOGs250m, global gridded hydrologic soil groups for curve number-based runoff modeling. Scientific Data 5, 180091. https://doi.org/10.1038/sdata.2018.91 (accessed on 12 August 2021).

We used the annual global landcover map data from the Copernicus Land Monitoring Service [31]. The global annual landcover maps follow the UN-FAO Land Cover Classification System (LCCS) and contain 23 discrete classes. The updated 2015 classification has slightly higher accuracy in characterizing forest, cropland, and permanent water classes according to Buchhorn et al. [31]. We then clipped and reclassified the 2015 landcover map according to the description provided by the USDA-SCS as shown in Table 2 and assigned the corresponding curve number. Figure 4 shows the raster analysis process towards the creation of CN values.
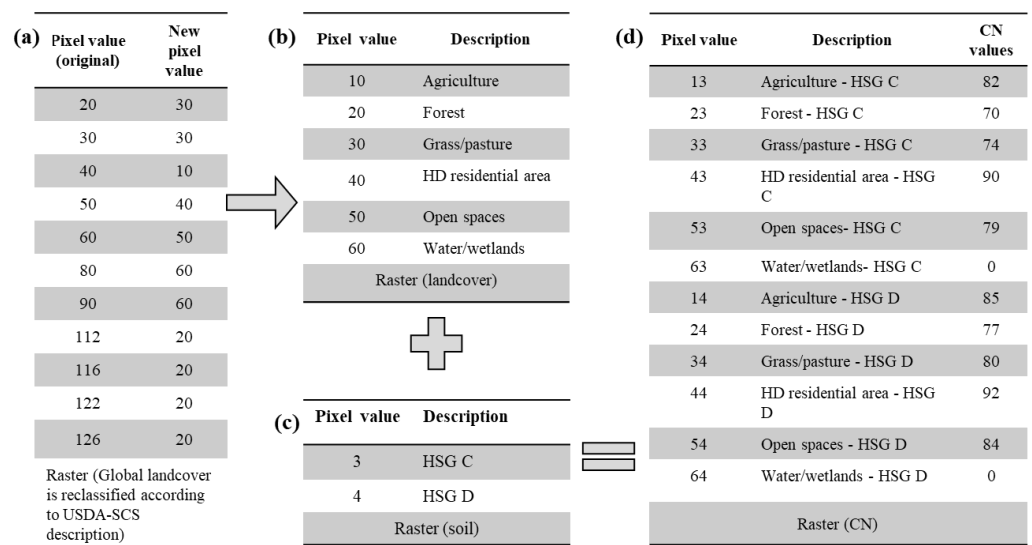
Figure 4. Process of CN raster creation from the landcover and HSG raster datasets. (**a**) The landcover raster is regrouped into landuses based on Table 2 and reclassified with new pixel values. (**b**) The reclassified landcover raster and its description. (**c**) The soil raster with its raster value added to the landcover raster in (**b**). (**d**) The sum of landcover and soil rasters reclassified according to the appropriate CN values of Table 2.

The information on the catchment area is needed to compute the discharge or flow rate at each site. The individual catchments were delineated using the identified sites as outlets within the SWAT watershed delineator. The catchment boundary and area, A_i in square meters, were computed. The catchment boundary was input to the Zonal Statistics of ArcGIS Spatial Analyst, which extracted the mean $\overline{q}_i$ raster values (in meters) within each catchment. We get twelve values (one for each month) of $\overline{q}_i$ for each site. The discharge at each site, Q_i in m^3/s, is computed using (4) where t_m is the number of seconds in a month.

$$Q_i = \overline{q}_i * A_i * /t_m \tag{4}$$

We used the 80% dependable flow value, the value used by NWRB-DENR [40] in its technical evaluation for hydropower projects. To get the 80% dependable flow, we constructed the flow duration curves (FDC) using the CN-estimated monthly runoff values for each potential site. With FDC, the monthly flow values were arranged in descending order, assigned the corresponding rank of 1 to 12 (1 for the highest monthly flow, 12 for the lowest flow), and computed the probability of flow exceedance using the equation,

$$p = 100 \ (M/(n \ + \ 1)), \tag{5}$$

where p, M, and n refer to the probability of exceedance (in percentage), discharge rank, and the number of events in a period, respectively. An example of a flow duration curve is shown in Figure 5.
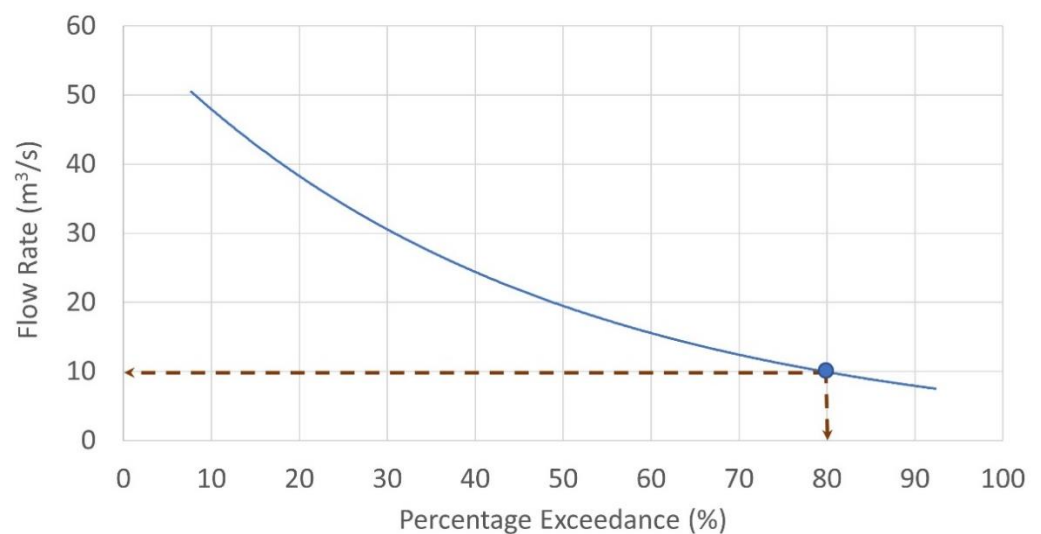
Figure 5. An example of a flow duration curve showing the equivalent flow of 10 m³/s at 80% flow exceedance.

We examined the actual flow record from an existing hydropower plant, the Loboc Hydroelectric Plant (LHEP), and the CN-estimated runoff. With the available data, we found no common years between the actual flow and the CN-estimated runoff. The flow data at LHEP spanned between 2005 to 2019. On the other hand, the CN-estimated runoff used a gridded precipitation dataset from the work of [32] based on precipitation records between 1970–2000. The different record years constrained us from comparing the actual and estimated runoff. In this case, the average patterns of the CN-estimated runoff and the local inflow data were presented instead.

2.4. Hydropower Capacity and Annual Energy Generation

The hydropower capacity, P_i (kW), is computed using the equation,

$$P_i = \eta \ \gamma \ H_{net,i} \ Q_{80net,i} \tag{6}$$

where η is the efficiency at 0.85 [41], γ (kN/m³) is the specific weight of water equal to 9.810, $H_{net,i}$ (m) is the net hydraulic head equivalent to 90% of the elevation head where 10% is allotted for frictional losses along the penstock, and $Q_{80net,i}$ (m³/s) is the net flow equivalent to 90% of the flow at 80% probability of exceedance where 10% returned to the waterway as environmental flow following the Philippines—National Water Resources Board Resolution No. 030613 [40] on the granting of water rights over surface water for hydropower projects. The sites' computed hydropower values were then classified according to Table 4.

Table 4. Classification of small-scale hydropower systems based on power capacity and the potential applications to a range of beneficiaries.

Type	Power Output [1,2]	Applicability [1]
Small	1–10 MW	Small communities with a possibility to supply electricity to a regional grid
Mini	100 kW–1 MW	Small factory or isolated communities
Micro	5–100 kW	Small, isolated communities
Pico	<5 kW	1–2 houses

[1] https://sswm.info (accessed on 20 July 2021). [2] [20,42].

The annual energy generation E_i at each potential site is computed using (7) where *CF* is the minimum capacity factor set at 33.73%, as considered by the Bohol Island Power Development Plan (BIPDP) [4], and *T* is 8760 h.

$$E_i = P_i \; CF \; T \tag{7}$$

2.5. River Profile Analysis

The topographic profile of a river system holds useful information of climatic and tectonic forcing across a landscape [43]. A river profile analysis demarcates locations of tectonic activity in tectonically active landscapes [44]. The study examined two geomorphometric indices: the knickpoints and the river steepness index.

The stream power model is widely used to describe the evolution of a river profile, e.g., [45,46], expressed as:

$$\partial z / \partial t = U\,(x,t) - E\,(x,t) \tag{8}$$

where $\partial z / \partial t$ is the change in elevation z {L} of a point in the channel that varies with time t {T} and distance x {L}, U {LT^{-1}} is the rock uplift rate, and E {LT^{-1}} is the river incision rate. At steady state, $\partial z / \partial t = 0$, indicating a balance between rock uplift and erosion. Rearranging Equation (8) and solving for *S* gives:

$$U = E = KA^m S^n \tag{9}$$

$$S = (U/(K\,A^m))^{1/n} \tag{10}$$

$$S = k_s A^{-\theta} \tag{11}$$

where Equation (9) defines the channel incision rate *E* [45] as proportional to the erodibility K {T^{-1}L$^{(1-2m)}$}, local slope S{L/L} and catchment area A{L^2}, and *m* and *n* are constants. Equation (10) describes a positive correlation between channel gradient and rock uplift rates [43] and assumes that river profiles developed over areas with similar climate, lithology and uplift rates uplift [47]. The terms k_s and θ in Equation (11) refer to river steepness and concavity index, respectively, and where $k_s = (U/K)^{1/n}$ and $\theta = m/n$. Equation (11) expresses a power relation between *S* and drainage area *A*. A regression analysis of log (*S*) versus log (*A*) gives the concavity index value, which usually ranged between 0.35–0.6 for tectonically active mountains and 0.3–0.6 under normal conditions. A reference concavity index, θ_{ref}, is introduced to remove the effect of different catchment areas [43,47] and to determine the normalized river steepness index, k_{sn}, as:

$$k_{sn} = S/A^{-\theta_{ref}} \tag{12}$$

where θ_{ref} varies between 0.35 to 0.65. k_{sn} and *K* are dimensional coefficients whose dimensions depend on the value of θ and the value of *m* [47]. The factor k_s is equivalent to M_χ [47], also called the river steepness index, which is the slope of the integral solution to the stream power model, when the reference area, A_0, in Equation (13), is equal to one:

$$M_\chi = (E/K\,A_o^m)^{1/n} \tag{13}$$

M_χ is also used to demarcate regions with rapid rock uplift in tectonic geomorphology [22]. A study by Schwanghart et al. [22] evaluated M_χ with peak ground acceleration in the Himalayan regions after the 2015 Gorka earthquake and established that earthquake-triggered landslide damages to hydropower plants clustered in areas where M_χ is high. The current study used Topotoolbox to analyze k_{sn} of stream profiles to illustrate quantitatively the channel morphology and provide insights into the spatial dynamics of deformation along river channels [48] and adopted a commonly used θ value of 0.45.

Knickpoints are manifestations of perturbations along river channels [44]. In addition, knickpoints are indicators of landscape disequilibrium significant in engineering structures [23]. In TopoToolbox, [28] located knickpoints using the 'knickpointfinder' function that extracts sharp convex sections in the river profile.

In our study, we used both the k_{sn} and the knickpoints to determine the level of risk associated with potential slope failures that may affect the structural stability of hydropower systems. We used TopoToolbox [28] to extract k_{sn} and the knickpoints from a digital elevation model and did further analysis and visualization in a GIS platform. The study classified the k_{sn} (in $m^{0.9}$) values into five levels of risk using the natural breaks method as follows: 5—very low ($<19\ m^{0.9}$), 4—low (19–$59\ m^{0.9}$), 3—medium (59–$131\ m^{0.9}$), 2—high (131–$298\ m^{0.9}$), and 1—very high ($>298\ m^{0.9}$). Then, we overlaid the identified knickpoints on k_{sn}, and rendered to each knickpoint the corresponding risk level class of the matching k_{sn}.

To identify the risk level associated with each potential site, we drew a 200-m radius buffer region around each site and determined the presence of a knickpoint within the buffer. When two or more knickpoints were present within the buffer, we attributed the highest level of risk for the site.

2.6. Land Use and Population Analysis

National parks and equivalent reserves are 'valuable for economic and scientific reasons and as areas for the future preservation of fauna and flora' [49,50]. In the Philippines, renewable energy projects may be allowed within the protected area and located outside the strict protection zones [50] (Sec. 13). The protected areas were obtained from the World Database on Protected Areas (WDPA), downloaded from www.protectedplanet.net (accessed on 13 October 2021), and the Protected Areas Database of the Regional Office 7 of the Department of Environment and Natural Resources. The protected areas within the study area were clipped and overlaid on the identified potential sites. The available protected area dataset has no information on different zones, specifically on strict protection zones. In this case, all protected areas were considered as strict protection zones, and all the potential sites found within were excluded from the list.

In evaluating the population that the potential hydropower systems can serve, the 2015 Philippine Census of Population data was used. The population data at the barangay (village) level can be downloaded from the Philippine Statistics Authority (http://psa.gov.ph) (accessed on 5 August 2021). The administrative map at the barangay level was obtained from a GIS data repository PhilGIS (http://philgis.org) (accessed on 8 August 2021), and the maps' area attribute was used to compute the population density. Next, the number of households per unit area was calculated, wherein the average household size of 4.4 in 2015 [51] was utilized. A point vector datum, located at the center of each barangay polygon, represents households per area. Finally, the point vector data were used to interpolate and create a raster of household per area.

The next step was to determine the number of households present in the vicinity of each potential site. In the potential sites layer, we created a 200-m buffer around each site. Then, the layer was overlaid on the household per area raster. The Zonal Analysis of ArcGIS extracted the mean household density within the buffer. The number of households within the 200-m radius was calculated as the product of the mean household density and 12.566 hectares. In this paper, this parameter is called HH_{200m}.

The number of households (required for pico- and micro-hydropower systems only following Table 4) that each potential site could support was estimated using the country's electricity

consumption per capita of 696 kWh in 2014 WorldBank data (https://data.worldbank.org) (accessed on 22 August 2021). Using a capacity factor of 33.73% and the annual number of hours of 8760, a micro-hydropower type with a 5–100 kW capacity can support a community of 5–96 households. In contrast, a pico system (<5 kW) can provide enough electricity to a cluster of fewer than five households. This parameter is referred to as HH_{site} in this paper. The difference between HH_{200m} and HH_{site} is then obtained. A zero or a positive value indicates electricity-consuming households that can make hydropower financially viable. In contrast, a negative value indicates that the number of households within the 200-m radius of each site is not enough to make the hydropower system economically feasible.

2.7. Case Study Application in Bohol Island, Central Philippines

Bohol Island is in the Philippines' archipelago's Central Visayas region, as shown in Figure 6. The island province covers roughly 4117 km^2 and its highest elevation is at around 833 m (see Figure A2). A 2015 global landcover data has identified more trees with a top density of 30%, dominating the island's landcover of about 70%, as shown in Appendix A Figure A3. Agriculture and tourism are the primary drivers of the island's economy.

The island's climate falls under the 4th type of Corona's climatic classification having rainfall distributed evenly throughout the year, with distinct dry and wet seasons. The annual precipitation between 2000–2012 observed at Tagbilaran Station ranged from 1210 to 2273 mm. Meanwhile, Appendix A Figure A4 shows the spatial variation of precipitation on the island based on a global climate dataset [32].
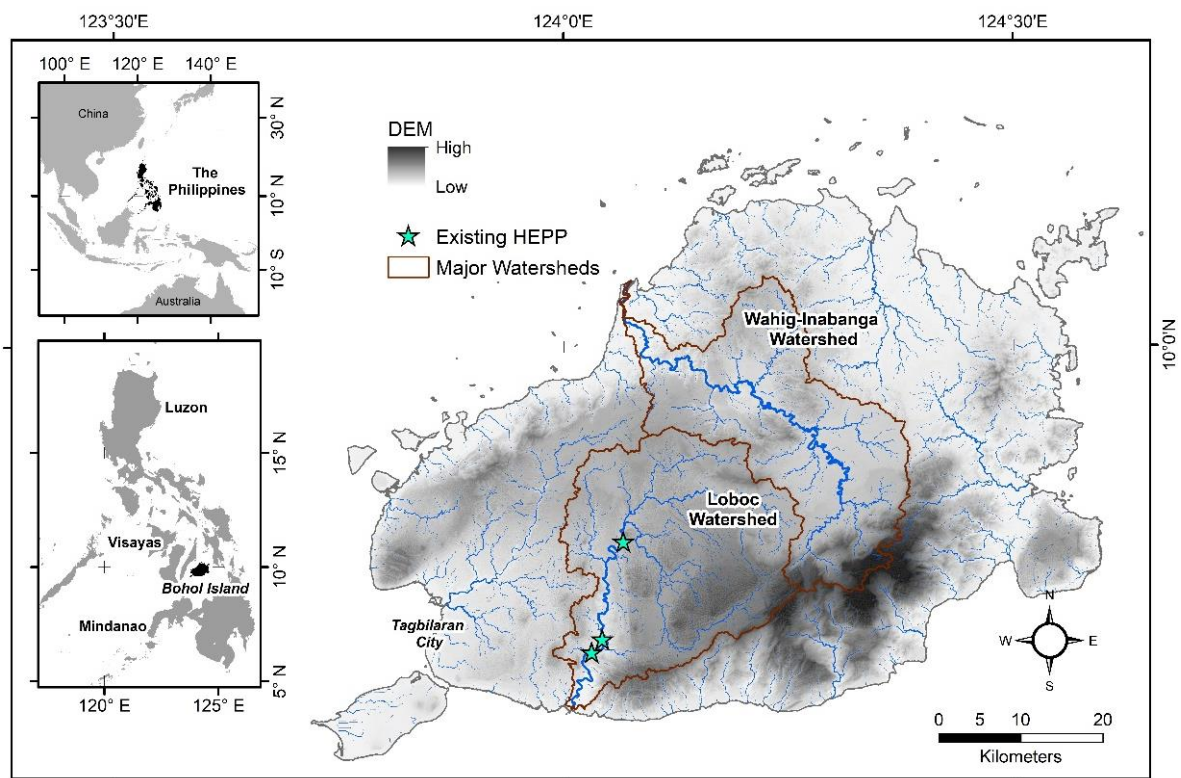
Figure 6. The Bohol Island, its drainage network, the three existing hydropower plants, and the major watersheds.

Based on the FAO-DSMW (Food and Agriculture Organization—Digitized Soil Map of the World) (WRB-IUSS, 2014), the soils in the island is dominated by three soil types consisting of orthic luvisols, dystric nitosols, and pellic vertisols. The luvisols are soils with clay-enriched subsoil. The nitosols are soil types with significant accumulation of clay (30 percent or more by mass and extending as much as 150 cm below the surface) and a

blocky aggregate structure. On the other hand, the vertisols are heavy clay soils with a high proportion of swelling clays. Regarding the hydrologic properties estimated from the global hydrologic soil groupings [52], the soils in the area are described as having moderately high to high runoff potential (See Appendix A Figure A5).

The island has two major watersheds: the Loboc and the Wahig-Inabanga Watersheds. All three existing run-of-river hydroelectric power plants are found in the Loboc Watershed along the main trunk: Sevilla mini HEPP, Loboc mini HEPP (LHEP), and Janopol HEPP (small HEPP) with a combined dependable capacity of 8.7 MW [52]. In 2015, these hydropower plants supplied around 11% of the island's peak energy demand of 77-MW while the Visayas Grid (Leyte–Bohol Transmission Interconnection) provided most of the island's energy needs [4].

Natural disasters such as typhoons and earthquakes regularly affect the island. In October 2013, a 7.2 magnitude earthquake destroyed physical infrastructure and cut off the island's energy supply for a few days to months. In the following month, the super typhoon Yolanda (with international code name Haiyan), although this time spared the island from further destruction, had wrecked the power transmission lines of nearby provinces from where Bohol receives most of its energy supply. Thus, power outages from the earthquake and typhoon interrupted energy-dependent activities and related activities, resulting in significant economic loss.

The unfortunate experience sent an urgent call for the Boholano people to plan and ensure sufficient power supply for the island if a natural catastrophe disengaged the province from the Visayas Grid [4]. To be more resilient to the effects of natural disasters, the government planned to put its energy generation plants in place. Hence, a resource assessment is timely to support the local government exploring potential renewable energy sources for energy self-sufficiency.

The province of Bohol has rich natural resources. While addressing the sustainable development goal of providing clean energy, renewable energy sources could ensure accessibility and availability of the needed energy, especially in rural areas. Rapid resource assessments and feasibility studies on potential hydropower generation sites were critical actions recommended by the Technical Working Group [4] to augment the power supply in the province. The assessment made by Pojadas et al. [42] found that the island's technical potential for domestic renewable energy resources, from any combination of solar PV, wind, biopower, and hydropower projects, can meet the 35% share of the renewable energy portfolio. On account of these resources and the natural disasters experienced by the island, the study assesses its hydropower potential incorporating landform dynamics following methods discussed previously.

3. Results

3.1. Landscape-Wide Topographic Analysis and the Potential Sites

Figure 7 shows the spatial distribution of small-scale hydropower sites identified for an island-wide topographic analysis along with the stream order. The topographic analysis identified 94 potential sites along river channels with a minimum elevation head of 20 m and higher. More than half of the identified sites are found outside of the two major watersheds. There are nine sites located along the main trunk of the Loboc Watershed, which already hosts the three existing hydropower plants. The potential sites are located at distances of more than 500 m from the existing hydropower plants. Other features of each site are given in Appendix B Table A1.

The elevation heads of the identified sites range from 20–62.4 m. Within this range, 71%, 19%, and 10% of the sites have elevation heads between 20–30 m, 30.1–40 m, and >50 m. The sites with elevation heads of 50 m and higher are in the Wahig-Inabanga Watershed (three sites), other watersheds (six sites), and the Loboc Watershed (one site).
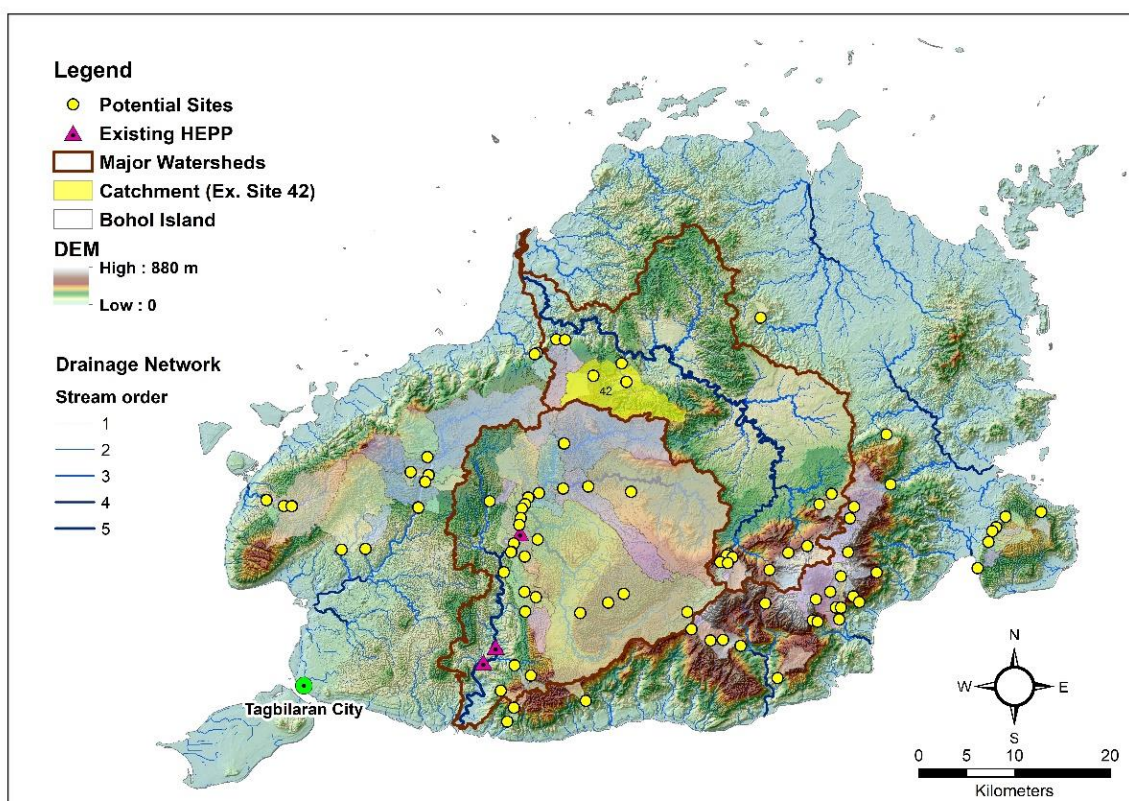
Figure 7. Spatial distribution of potential small-scale hydropower sites identified through topographic analysis, the stream order, corresponding catchment, and the drainage network.

The potential sites fall under different stream orders that vary with elevation heads and catchment areas, as shown in Figure 8. Using Strahler's stream ordering system, five stream orders are identified in the study area. The longest river, a fifth-order stream, has a total length of 83.3 km but no potential site is found. More than half of the sites (or 52%) are found in the first-order streams, while only four are in the fifth-order streams. The number of potential sites decreases with increasing stream order. A similar trend was found in the study of [16] in the Taw at Umberleigh catchment of South West England where more than half of the detected locations are found in the first-order channels, and the number decreases as the channel order increases. Twelve sites with third-order streams have the highest average elevation head of 36.4 m, while five with fourth-order streams have the lowest average elevation head of 22.8 m. Results indicated no correlation between stream order and elevation head. Four sites found in fifth-order streams have the highest average catchment area of 473 km^2, while more than half of the identified sites have first-order streams with an average catchment area of only 2 km^2. The sites' catchment areas increase with stream order.

3.2. Runoff Estimates

Figure 9 shows the spatial variation of the annual and monthly runoff in the study area, including the annual precipitation. Based on a global dataset [32], the mean annual precipitation varies from 1537 mm to 2263 mm, with the westernmost coast as the driest part and the high-altitude southern portion as the wettest part of the island. The average annual runoff depth varies across the landscape from 657 mm to 1941 mm, or 43% to 87% of the annual precipitation becomes runoff, increasing from the east towards the interior part of the island. The monthly variation of runoff indicates April as the driest month, while November is the wettest month.
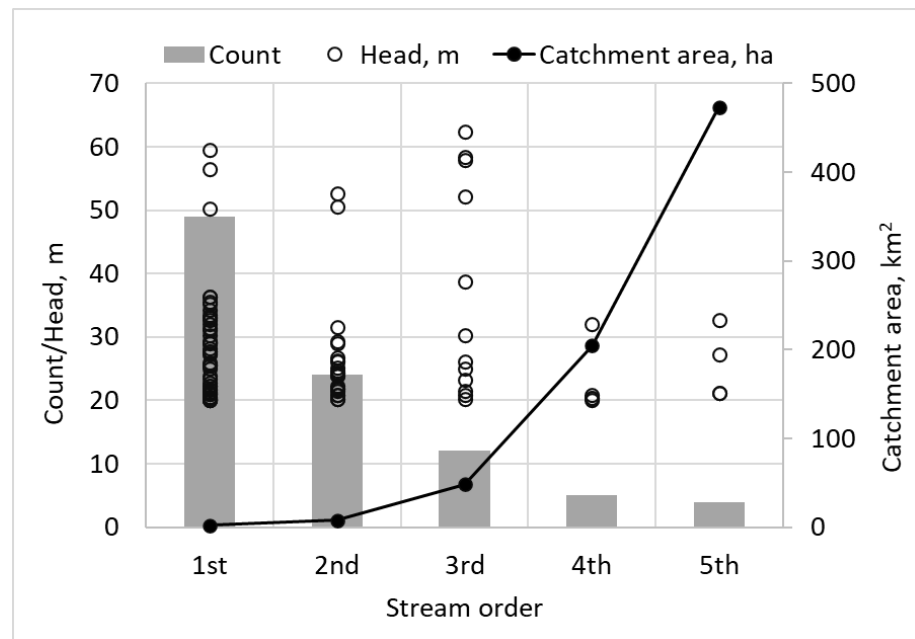
Figure 8. The number of sites, elevation head, and average catchment area of the identified potential small-scale hydropower sites under different stream orders.
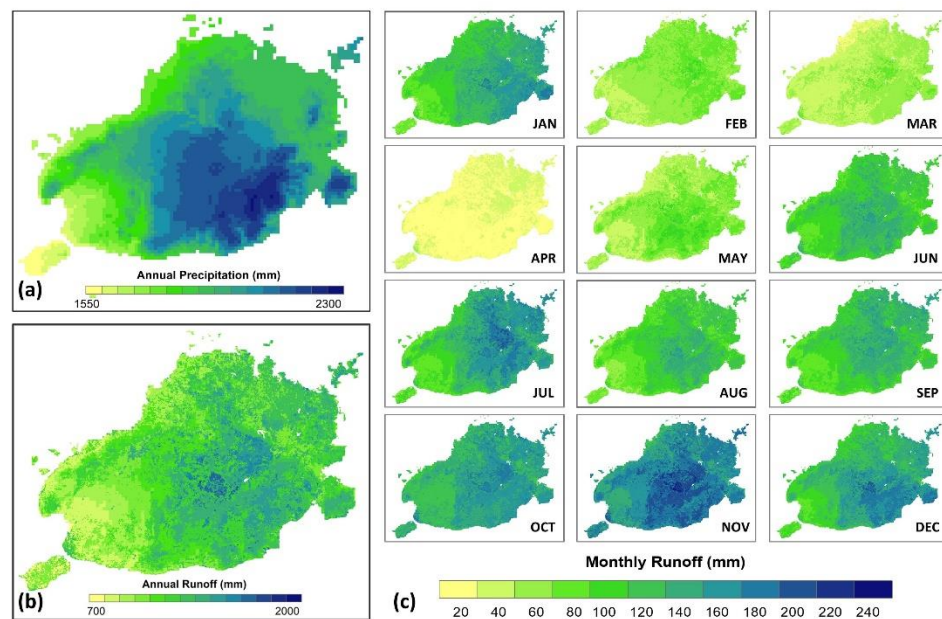
Figure 9. Spatial variation of (**a**) mean annual precipitation, (**b**) mean annual runoff depth, and (**c**) mean monthly runoff estimated using CN method.

Figure 10 shows the relationship among flow estimates, catchment area, and stream order. The average catchment area and the average flow estimates increase with increasing stream order (Figure 10a). Earlier, Figure 8 shows fewer potential sites are identified in higher order streams, and more than half are in the first-order stream. Zooming in on the flows under the first-order stream, we found flow increasing linearly with the catchment area (Figure 10b). However, in Figure 10c, several potential sites concentrated at the bottom left side of the graph and depicts a reduced linear relationship between the catchment area and flows compared to the general relationship using all the potential sites in this stream order.
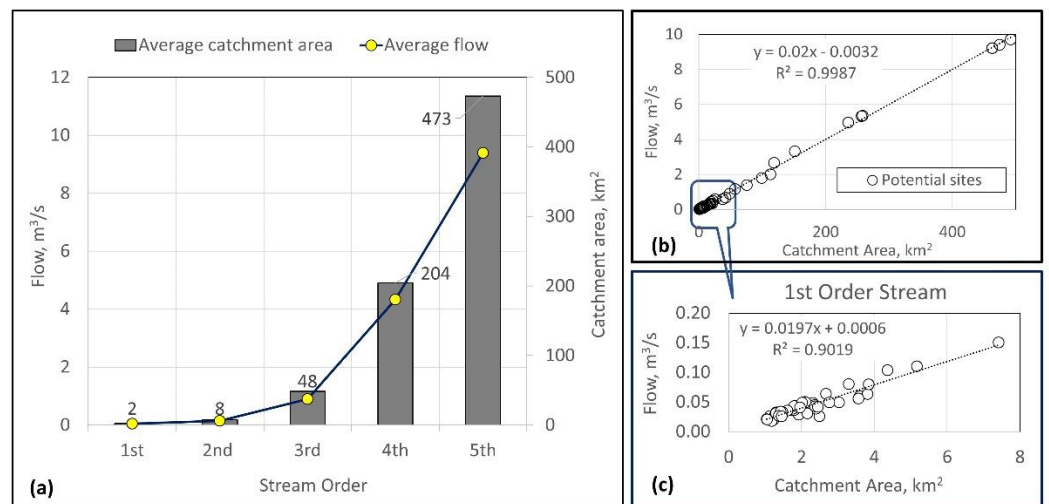
Figure 10. Flow estimates, stream order, and catchment area of the identified sites. (**a**) Average catchment area and flow by stream order. (**b**) Flow-catchment area relationship under first-order stream. (**c**) First stream order potential sites' flow-catchment area relationship.

The observed flow data and the estimated runoff using the CN method at the LHEP station, both expressed in mean daily values, are shown in Figure 11. Though both flow datasets show the lowest daily runoff in April, the month with the highest daily flow was November based on CN method estimates. With the actual flow observation, the highest flow was recorded in January. The two runoff curves are showing different patterns: the CN estimated flow shows a more erratic annual pattern with a minimum, maximum and average values of 2 m^3/s, 33 m^3/s, and 19 m^3/s, respectively, while the observed flow at LHEP is smoother with the minimum, maximum, and average flows of 9 m^3/s, 18 m^3/s, and 14 m^3/s, respectively. However, considering the annual 80% dependable flow for a year, the CN flow estimate is lower by 0.56 m^3/s.
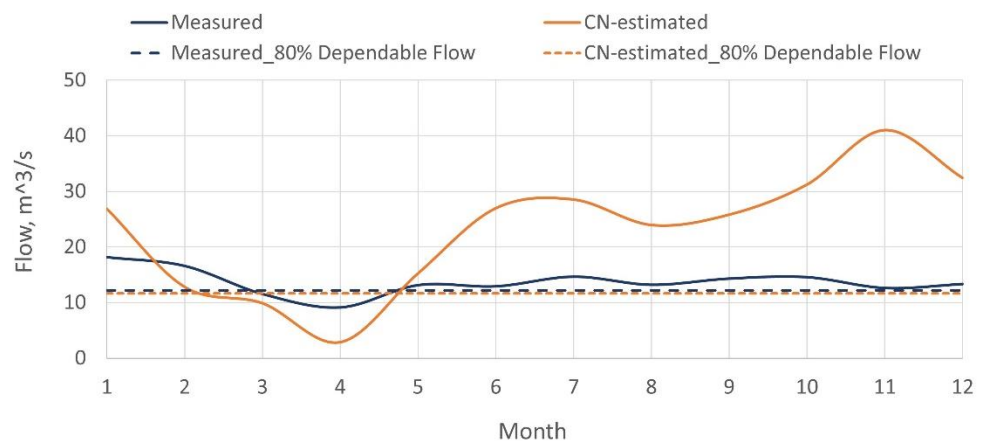
Figure 11. Observed and estimated flow at the LHEP site. The potential hydropower computation uses the flow value estimated by the CN method at 80% dependability.

3.3. Potential Power and Energy Generation

Table 5 summarizes the potential sites' count, power, and energy generation for each watershed. Section 3.1 presents the distribution of sites per watershed. The power capacity and energy generation are highest in Loboc Watershed, with 75% of the total. It is followed by 21% from other watersheds and 4% from the Wahig-Inabanga Watershed. All the four small types are found in the Loboc Watershed, which has a total power capacity of 6.5 MW accounting for 48% of the total power. Most of the sites are found in smaller

watersheds, with 5 mini and 39 micro types having a total power capacity of 2831 MW accounting for 21% of the total power capacity. Although the Wahig-Inabanga Watershed is the second-largest catchment, only a few potential sites are found in the watershed with smaller power capacities.

Table 5. Types of small-scale hydropower sites, count, power capacity, and energy generation per watershed.

Watershed	Type	Power, kW	Count	Energy, MWh
Loboc Watershed		10,169	29	30,045
	Small	6484	4	19,159
	Mini	3354	6	9911
	Micro	316	15	934
	Pico	14	4	42
Wahig–Inabanga Watershed		569	15	1682
	Mini	356	1	1051
	Micro	200	11	592
	Pico	13	3	40
Other Watersheds		2857	50	8441
	Mini	1979	5	5846
	Micro	853	39	2520
	Pico	25	6	75

Small (1–10 MW); mini (0.1–1 MW); micro (5–100 kW); and pico (<5 kW). Please see Appendix B Table A1 for details per site.

The number of potential sites in the study area is dominated by micro types followed by pico, mini, and small types, having 69%, 14%, 13%, and 4% of the total count. Although the micro types lead in terms of number, they only contribute 10% to the total annual energy generation since each site can generate around 62 MWh on average. In terms of total power capacity per type, the major contribution comes from four small types contributing 48%, while 12 mini types share 42% of the total power capacity.

3.4. Geo-Hazard Risks Associated with Each Potential Sites

Table 6 shows the classification of the potential sites according to geo-hazard risk level, while Figure 12 depicts the spatial distribution and the associated risk. Potential sites with 'high to very high' risk levels comprise 74% (70 out of 94 sites), supplying 18% of the total potential power. Most of the micro types are found under this risk level, with 55 out of 65 micro sites. Meanwhile, the sites with 'low to very low' risk levels are 16% of the total sites and contribute 52% of the total potential power. There are nine sites with 'medium' risk levels which provide about a third of the total potential power. On the other hand, a quarter of the total potential power comes from two small types in low-risk areas.

The map in Figure 12 shows the spatial distribution of the 94 potential sites, the type indicated by the size of each bubble, and the associated risk level indicated by the color. In the Loboc Watershed, there are 17 sites exposed to 'high to very high' risk levels that contribute 12% to the total power capacity, including a small type with a capacity of 1.341 MW. The other three small types found inside the watershed are under 'low to medium' risk levels with an aggregate capacity of 5.143 MW. Inside the Wahig-Inabanga Watershed, 14 of the 15 sites are under 'high to very high' risk levels. One mini type, located downstream of the watershed, is classified under 'very low' risk level. The remaining 50 sites located outside of these 2 watersheds are under different risk levels. There are 21 and 18 sites with 'high' and 'very high' risk levels, respectively, where 32 sites are micro types.

Table 6. Geo-hazard risk levels associated with the small-scale hydropower type and the power potential.

Geo-Hazard Risk Level	Type	Number of Sites		Hydropower	
		Count	Total	Power, kW	Total
Very high	Mini	1	32	676	907
	Micro	31		231	
High	Small	1	38	1341	1591
	Micro	24		197	
	Pico	13		53	
Medium	Small	1	9	1790	4078
	Mini	4		2209	
	Micro	4		80	
Low	Small	2	5	3353	3895
	Mini	1		411	
	Micro	2		131	
Very low	Mini	6	10	2837	3122
	Micro	4		285	
Total		94		13,595	
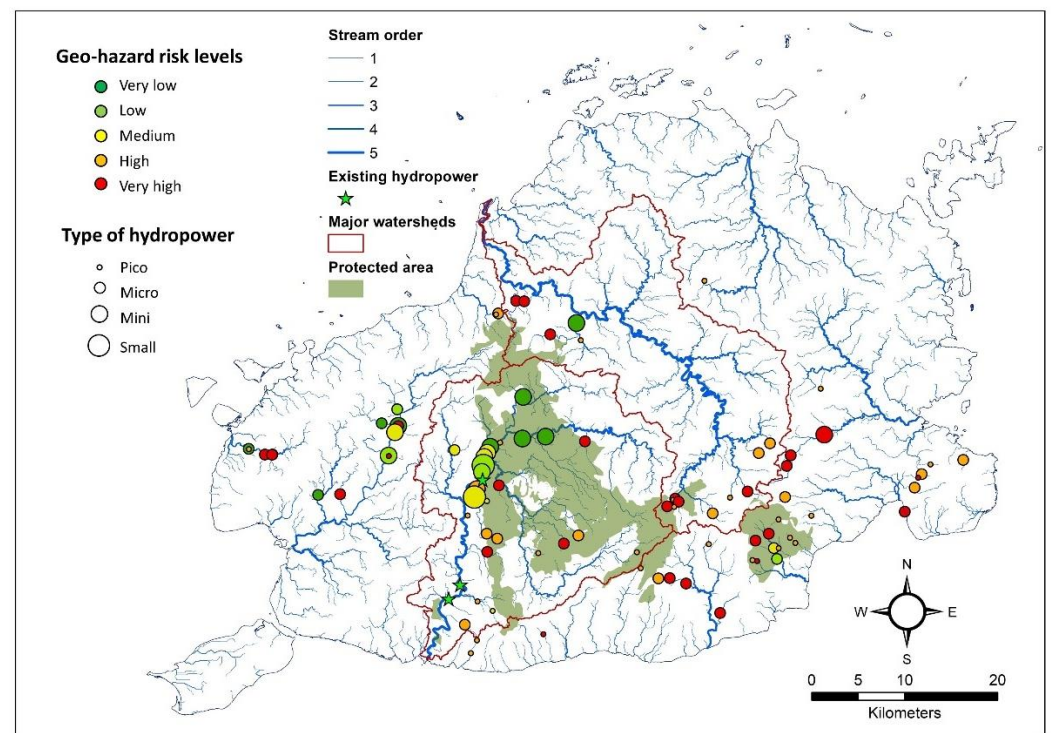
Figure 12. Spatial distribution of the 94 potential small-scale hydropower sites, their types and the geo-hazard risk levels, and the protected area.

3.5. Land-Use and Population Constraints

The protected areas in the study area's mainland, depicted in Figure 12, cover 35,016 hectares as promulgated by the Philippine Law [50]. The same legal instrument indicated that hydropower projects within protected areas are allowed but preferably outside of the strict protection zones and upon the approval of authorized agencies. However, the available dataset does not specify the specific zones within the protected areas, especially

the strict protection zones. With this limitation, the study assumed that the protected areas are the strict protection zones and, hence, excluded all potential sites found inside the protected areas.

There are 35 potential sites inside the protected areas, accounting for 37% of the total sites and 53% of the total potential power capacity. Of the 35 sites, 22 are micro types with an aggregate power capacity of only 402 kW. Inside the protected areas are found two small and seven mini types, which account for 50% of the total power capacity, and one of the existing hydropower plants.

The population analysis targets the pico and micro types. Due to the limited capacities of these hydropower types, certain household number should be present in the vicinity of the site to minimize the cost of putting up transmission lines [53]. The household analysis found 27 sites fail to show the required household number within a 200-m radius. Hence, there are 25 potential sites left after land-use and population constraint analysis. The remaining power capacity is now reduced to 40% of the total. Six sites inside the Loboc Watershed provide 58% of the remaining power capacity. A total of 64% of the remaining sites are found outside the two major watersheds with 36% power capacity. In contrast, the three sites inside Wahig-Inabanga Watershed contribute only 7% of the power capacity.

4. Discussion

The hydropower potential of a landscape is driven by the dynamics of its topography and hydrology: topography provides the hydraulic head while the hydrology provides the discharge rate information. Characterizing these features of the landscape will help us to understand the potential of the available resource [54] particularly for hydropower generation. Such landscape characterization also enables the identification of geo-hazard risks associated with each site enabling the development of location-specific engineering designs or the prioritization of sites for further development [23]. The dynamics of a landscape is also, in one way or another, impacted by anthropogenic influences which can further restrict potential resource use in favor of environmental concerns as well as economic considerations.

4.1. Loboc Watershed Hydropower Potential and Environmental Concerns

Most of the hydropower potential in the island landscape of Bohol, Philippines, can be harnessed within the Loboc Watershed. About three-fourths of the estimated hydropower (or 10.2 MW) can be generated from the sites identified inside the watershed, mainly along the main trunk where the three existing hydropower systems are found. The nine potential sites found in the Loboc River can possibly augment the three existing hydropower plants currently having a total installed capacity of 8.7 MW [4]. Tamm and Tamm [20] also found new suitable sites along Estonian rivers where hydropower has been or is currently harvested. However, the identified potential sites suggest a series of small-scale hydropower projects. In this kind of arrangement, Mayor et al. [9] cautioned that such systems would result in a "cumulative environmental impact cascading along the river system". Their study suggested reducing the number of low-capacity systems with less significance to the final energy generation and optimizing the use of existing hydropower infrastructure by integrating pumping and storage technologies.

The Loboc Watershed is also an area of high biodiversity value where 40% of its land area is declared protected (see Appendix A Figure A5). About 77% of the protected areas in the mainland of Bohol are inside the watershed covering the Loboc Watershed Forest Reserve and the Chocolate Hills Natural Monument [49,50]. Section 13 of Ref. [50] restricted renewable energy projects within strict protection zones of the protected areas. However, as of the conduct of the study, data defining the strict zones inside the protected areas were not available. Given the situation, we applied the restrictions inside the whole protected areas, similar to a study of [16], and found only two of the nine sites on the main Loboc River to be developable. In the study of Sammartano et al. [16] in the Taw at Umberleigh catchment (South West England) all sites within protected areas

were excluded due to environmental and economic issues. The UK Environment Agency required potential sites located within protected areas to secure permits and only the sites with well-designed measures preventing negative impacts may be allowed [16]. Integrating the best measures to ensure environmental integrity will entail higher investment cost to realize a hydropower plant [16].

4.2. Potential Sites Outside of Major Watersheds

The topographic analysis using a DEM, which covers the whole landscape, has identified more than half of the total potential sites outside the two major watersheds in the study area. These potential sites dispersed across the study area present an opportunity for remote areas to harvest hydropower, take advantage of the available resource, and provide power to small communities and small-agro industries, as documented in several studies [53,55]. The study results provide a new perspective on assessing a landscape for potential small-scale hydropower sites to encompass all watersheds irrespective of scale. In the initial assessment of an area for potential hydropower site exploration, such an approach is critical, giving insights into the overall hydropower potential of an island landscape. Further work to improve on this new approach, including the validation of the identified sites (ex. [16,20]), is suggested in future studies.

4.3. Small-Scale Hydropower Potential in the Island Landscape

The results of power capacity analysis showed that harnessing the hydro-based renewable energy sources in the study area will comprise several small-scale units distributed throughout the main island. However, there are contrasting feedbacks on the deployment of many small-scale hydropower systems due to environmental impacts and other issues (e.g., [9,53]). But for the Italian case where large-scale systems were already developed and suitable sites were already utilized, it was emphasized that increasing hydropower contribution could come from small-scale systems [56]. Moreover, many of the small-scale hydropower systems benefit rural development [8,53,55]. The advantages of these systems to rural areas in developing countries include improvement in productivity, women empowerment through energizing small agro-industries, and the notable little environmental impact. On a side note, small-scale hydropower systems are also challenged with high initial costs [55], but such can be counteracted by little operation and maintenance costs.

Notably, the study limits the potential sites to a minimum elevation head of 20 m. Future studies may consider a lower elevation head (<20 m) to identify potential hydropower sites. The global hydropower assessment of Hoes et al. [2] sets a minimum elevation head of 1 m but limits the river discharge to 0.1 m^3/s to deliver the smallest hydropower plant capacity of 1 kW, while the study of Arthur et al. [35] considers 10 m as the minimum head in its final selection of hydropower sites.

4.4. Dataset Limitations

One of the challenges in resource assessment for many developing countries is the limited historical climate datasets, flow data, updated landcover, and soil hydrologic properties of a target landscape [13,57]). The study demonstrated the use of global datasets to estimate runoff from hydrologic soil group data, gridded precipitation data, and landcover datasets in the initial assessment phase. Several similar studies used global datasets such as the FAO digital soil map of the world to carry their analysis (ex. [35]). However, the study results still call for localized data to validate the estimated runoff and establish the efficiency of the CN method in estimating runoff for the target landscape. Furthermore, it would also be interesting to use physically based hydrologic models such as the studies of [16,18,35,58] to improve understanding of the hydrology of the study area. Further fieldwork such as those conducted by [16] is necessary to validate the results.

4.5. Geometric Index of Geo-Hazard Risk

The river profile analysis from a digital elevation model was employed to quantify the geo-hazard risk level associated with each potential site, using the geometric index k_{sn} and knickpoints. The analysis gave insights on tectonically active areas in the landscape as manifested by the river channels' high river steepness index and presence of knickpoints, thus indicating the landscape's vulnerability to tectonic activity. A positive correlation of k_{sn} with uplift rates, and the arrangement of knickpoints are indications that a landscape is temporarily reacting to regional uplift along the subduction zone as what Boulton et al. [26] found in the Makira, Solomon Islands. Further, the study [26] suggested that the formation and propagation of knickpoints was generated by an increase in uplift rates and the associated base-level fall. A study by [22] found severe damages to hydropower projects as primarily caused by earthquake-triggered landslides in the Himalayan region during the 2015 Nepal's Gorkha earthquake, and also revealed the landslides clustered in areas with high values for river steepness index and ground peak acceleration. Upon evaluation using seismic hazard and river steepness, the study [22] predicted most of the Himalayan rivers were unsuitable for hydropower projects. In their study, it was emphasized that hazard assessment for hydropower projects must consider both seismic and geomorphic settings of potential sites. Landform dynamics indicated by geomorphic indices, proxies of tectonic and climatic processes, are crucial for engineering structures that sit on transient landscapes as emphasized in the study of Geach et al. [23] Channel stability, according Schwanghart et al. [22], is a primary concern where hydropower structures are usually situated along or adjacent to 'steep river channels and towering sidewalls' that are disposed to become unstable during strong seismic activity.

The integration of geomorphic indices in the initial assessment of land resources for small-scale hydropower sites allow for classifying potential sites according to geology-related hazards. The classification maybe a useful tool to assist decision-makers and project developers to prioritize potential sites for further development. The study by Geach et al. [23] produced a geohazard constraint map showing ground related hazard. The maps are expected to provide guidance to the project crew in conducting field investigations, designing location-specific construction methodologies and in addressing ground limitations [23].

The current study, however, is limited to two geometric indices only. Future work may consider other metrics of surface and geology-related processes relevant to hydro-related structures such as those in the studies of [22,23]. The availability of landslide records in the study area may reinforce the usefulness of the river profile analysis in the initial assessment phase of hydropower development.

4.6. Land-Use Policy and Population Density as Constraints

Land-use classifications posed limitations to hydropower projects as promulgated by legal instruments. Existing land-use policy limits hydropower projects within 'strict zones' of protected areas [59]. Due to limited information on the zoning within declared protected areas, the study has considered the whole protected areas as strict zones, removing several potential sites. Meanwhile, the presence of end-users near potential sites is an indicator of project economic feasibility, specifically for micro and pico hydropower types. For these types, a minimum number of households that clusters near a potential site is a requirement to keep the cost of transmission low [3,53].

The constraint analysis, examining land use and population, has significantly reduced the number of potential sites by 73% and consequently the potential hydropower capacity by 60%. However, these two issues can be viewed as temporary constraints and are expected to change in the future. With the country's increasing population, there is a tendency that areas devoid of communities may later be encroached with clusters of households that need hydro-based energy sources to support their economic activities, turning the identified potential sites to be more economically viable. On the other hand, planning authorities may soon refine and precisely define zones under strict use within the protected areas. Once

this happens, potential sites located in the protected areas but not in strict zones can be developed, thus, optimizing the hydropower potential found in the landscape.

As the economy develops, the demand for more energy to drive economic activities increases. It has been shown that energy generation significantly contributes to global warming and environmental impacts [6,7]. One way forward is to explore for lesser impacts and shift towards renewable energy sources, integral for a sustainable future. In many developing countries where land and water resources are available, the exploitation of hydropower sources is an attractive prospect [3,7]. Such systems offer less impact on the environment than fossil-fueled energy production, but initial investment cost seems high [3,7,35,54]. Knowledge of the possible adverse effects of hydropower and the underlying cost effectiveness are a challenge to future decisions on the scale of new developments. However, small-scale hydropower systems are still an alternative where the large-scale hydropower systems are no longer feasible or are already explored [60]. Other renewable sources such as geothermal, biomass, wind, and solar are other options to explore.

5. Conclusions

The resource assessment for hydropower site identification is usually limited to major watersheds identified in each landscape. A landscape's topography and hydrology are examined using GIS, terrain analysis tools, and hydrologic models to understand watershed parameters necessary to identify suitable locations and estimate hydropower capacity. Moreover, local datasets needed to carry out the analysis are usually not available or are limited. Advanced tools and the freely available global datasets enable the characterization of landscape dynamics for potential hydropower sites. An equally important factor to consider in the site exploration is the risk to geo-hazard and other surface processes in tectonically active landscape. Further, existing land-use policy in relation to environmental concerns and a population analysis posed as constraints to limit the identified potential sites. We applied the foregoing method in the island landscape of Bohol, the Philippines, and drew the following conclusions:

(a) The approach employed in the study reveals potential small-scale hydropower sites inside major and small watersheds. More than half of the identified sites are located outside the major watersheds, with a share of about 21% of the total potential power capacity;

(b) Freely available global datasets are successfully used to estimate runoff using the CN method and found runoff varying spatially and temporally across the landscape and at each potential site;

(c) The hydropower potential in the study area consists of a range of small-scale hydropower systems with different power and energy generation capacities. In terms of number, the micro types dominate in the study area, but four small types provide almost half of the potential hydropower;

(d) Each potential site is found under varying levels of geo-hazard risk innate to the geography and geology of the area. Seventy-four percent (74%) of the sites are under 'high—very high levels' of geo-hazard risk, while 52% of the total potential power capacity can be produced from low-risk sites;

(e) The land-use and population analysis found several potential sites inside protected areas and in areas where the number of beneficiaries is still limited. The analysis result reduces the number of sites by 73%, and consequently, power capacity by 60%. Future changes in land-use planning and an increase in population in remote areas are seen to optimize the development of the identified potential sites;

(f) The study produced decision-support maps showing the potential sites' spatial distribution, the hydropower types and power capacities, and the risk levels associated with each site. The maps are expected to provide crucial information for resource managers and decision-makers.

In summary, the approach used, and the results presented could be valuable support tools for decision-makers and energy developers in identifying potential sites for small-scale hydropower in the study area during the initial assessment phase of hydropower exploration.

Appendix A

Figure A1. A detailed flow of analysis for the study.
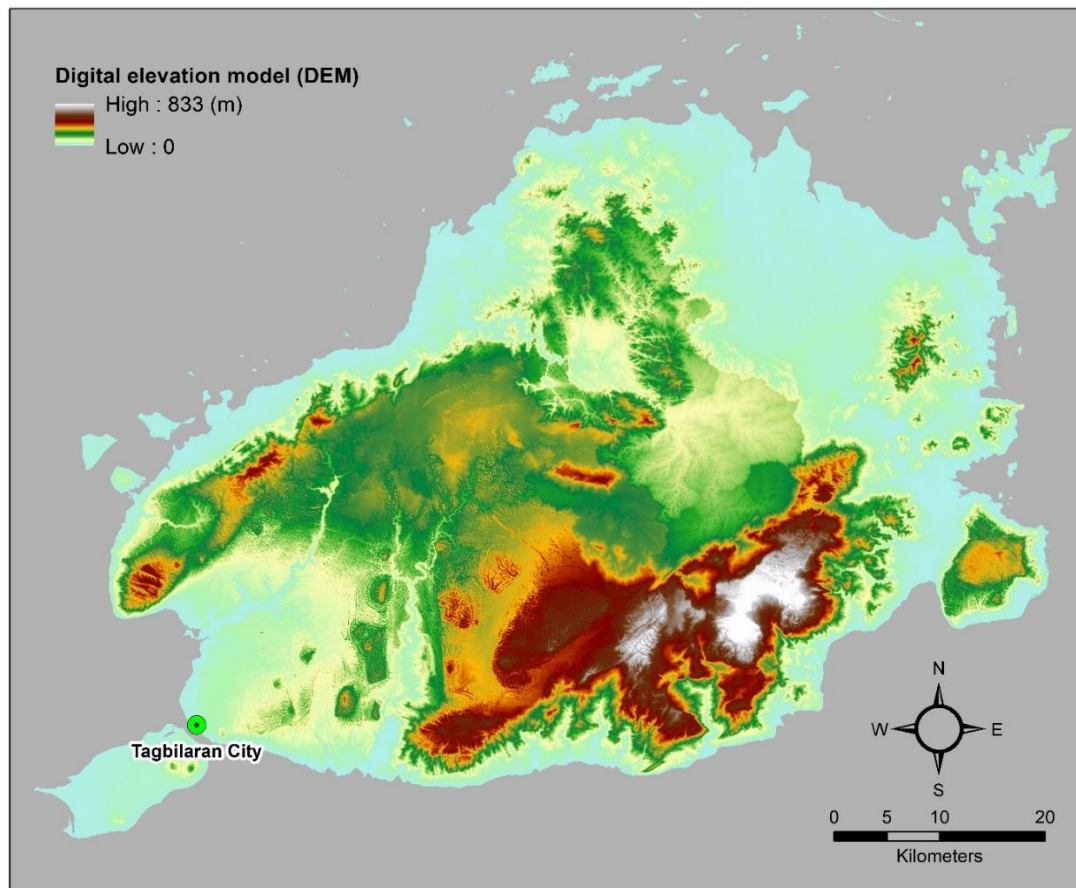
Figure A2. A digital elevation dataset of the study area.

Code	Landcover Class	Description
10	Cultivated land	It refers to the lands used for cultivating crops. Paddy fields, irrigated upland, rainfed upland, vegetable land, cultivated pasture, greenhouse land, land mainly planted with crops rarely with fruit trees or other trees, tea garden, coffee garden, and other economic cropland and so on are included in this category.
20	Forest	It refers to the lands covered with trees, the top density of which occupies over 30%. Deciduous broadleaf forest, evergreen broadleaf forest, deciduous coniferous forest, evergreen coniferous forest, mixed forest and sparse woodland the top density of which covers 10%–30% are included in this category.
30	Grassland	It refers to the lands covered by natural grass with cover density over 10%. The prairies, meadow steppes, alpine grasslands, desert steppes and lawns etc. are included in this category.
40	Shrubland	It refers to the lands covered with shrubs and the cover density over 30%. Mountain shrubs, deciduous and evergreen shrubs, and desert jungle in desert area with the cover density over 10% are included in this category.
50	Wetland	It refers to the junction lands of land and water area, which are constantly covered by biogas or hygrophyte plants and shallow water or wet soils. Inland marsh, lake marsh, river floodplain wetland, forest/shrub wetland, peat bogs, mangrove, salt marsh etc. are included in this category.
60	Water bodies	It refers to liquid water covered region in the land area. River, lake, reservoir, pit-pond etc. are included in this category.
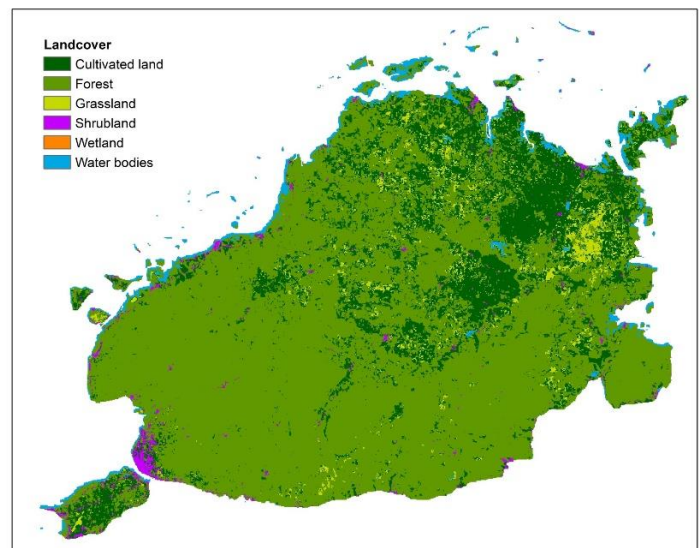
Figure A3. Details of the landcover in the study area.

Mean Monthly Precipitation (mm)

Mean Annual Precipitation (mm)
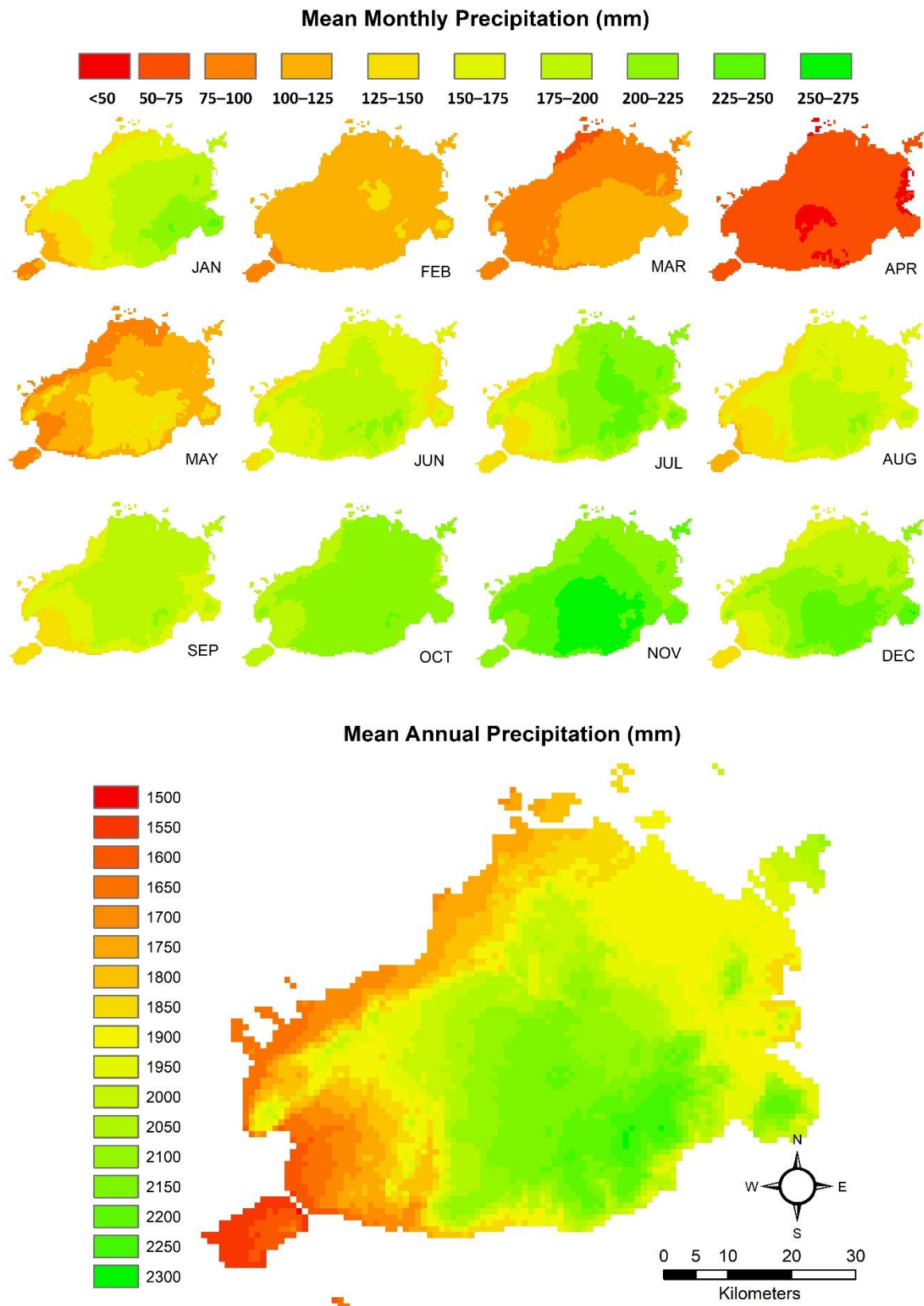
Figure A4. Temporal and spatial variation of precipitation in the study area.

Pixel values	Description
3	HSG-C: moderately high runoff potential (<50% sand and 20–40% clay)
4	HSG-D: high runoff potential (<50% sand and >40% clay)
13	HSG-C/D: high runoff potential unless drained (<50% sand and 20–40% clay)
14	HSG-D/D: high runoff potential unless drained (<50% sand and >40% clay)
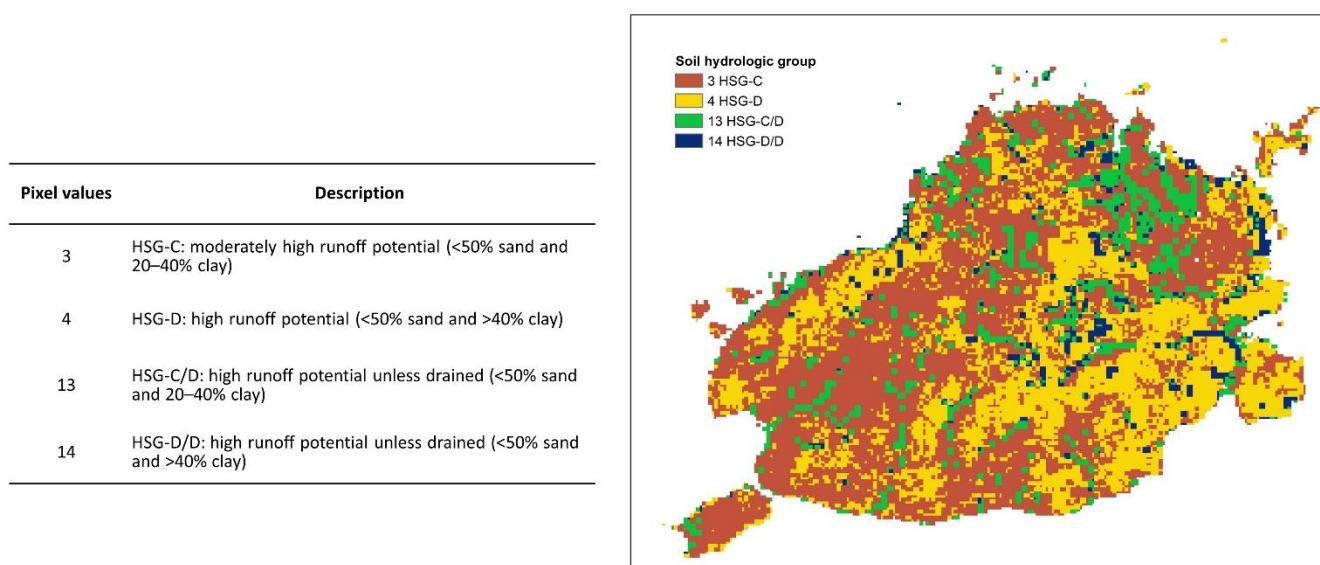
Figure A5. Spatial variation of the hydrologic soil group in the study area.

Appendix B

Table A1. List of potential small-scale hydropower sites identified in Bohol Island, Philippines.

Count	Watershed	Catchment ID	Area, ha	Gross Head, m	Flow, m^3/s	Power, kW	Annual Energy, kWh	Type	k_{sn} Class	HH_{200m}	HH_{site}	HH_{diff}	Protected Area
1	Other	1	148	20.6	0.029	4	11,976	pico	high	4.6	3.9	0.7	outside
2	Wahig-Inabanga Watershed	4	1211	24.4	0.212	35	103,096	micro	very high	2.8	33.7	−30.9	outside
3	Wahig-Inabanga Watershed	13	360	35.6	0.060	14	42,357	micro	very high	8.2	13.8	−5.6	outside
4	Other	19	219	31.4	0.041	9	25,648	micro	high	4.5	8.4	−3.8	outside
5	Other	25	250	31.0	0.026	5	15,853	micro	high	3.8	5.2	−1.3	outside
6	Wahig-Inabanga Watershed	42	4867	58.4	0.902	356	1,050,624	mini	very low	0.0	0.0	0.0	outside
7	Wahig-Inabanga Watershed	45	716	26.7	0.127	23	67,614	micro	very high	6.3	22.1	−15.8	outside
8	Wahig-Inabanga Watershed	53	118	32.0	0.022	5	14,033	pico	high	6.0	4.6	1.4	outside
9	Other	60	114	29.3	0.026	5	15,254	micro	high	3.6	5.0	−1.4	outside
10	Loboc Watershed	63	748	20.8	0.135	19	55,978	micro	very high	2.8	18.3	−15.5	inside
11	Loboc Watershed	65	5722	20.9	1.168	165	488,058	mini	very low	0.0	0.0	0.0	inside
12	Other	68	1643	24.8	0.303	51	149,926	micro	very low	8.6	49.0	−40.4	outside
13	Other	71	1759	20.2	0.322	44	130,025	micro	low	8.6	42.5	−33.9	outside
14	Other	80	1303	31.6	0.232	49	146,047	micro	very low	5.5	47.7	−42.2	outside
15	Other	85	7598	62.4	1.398	589	1,739,438	mini	very low	0.0	0.0	0.0	outside
16	Other	90	382	59.6	0.063	25	75,141	micro	very high	7.3	24.5	−17.2	outside
17	Other	103	356	56.5	0.056	21	62,982	micro	very high	5.5	20.6	−15.1	outside
18	Other	113	9965	52.1	1.801	634	1,873,906	mini	medium	0.0	0.0	0.0	outside
19	Other	116	2526	57.9	0.591	231	682,922	mini	very high	0.0	0.0	0.0	outside
20	Loboc Watershed	125	11,876	32.1	2.661	576	1,702,843	mini	very low	0.0	0.0	0.0	inside
21	Loboc Watershed	130	15,174	20.9	3.325	469	1,385,436	mini	very low	0.0	0.0	0.0	inside
22	Loboc Watershed	137	994	23.8	0.203	33	96,352	micro	very high	7.3	31.5	−24.1	inside
23	Loboc Watershed	139	124	21.0	0.021	3	8644	pico	high	3.9	2.8	1.1	inside
24	Wahig-Inabanga Watershed	141	277	24.4	0.065	11	31,791	micro	high	7.5	10.4	−2.9	outside
25	Loboc Watershed	147	1899	21.5	0.327	47	140,209	micro	very high	4.5	45.8	−41.3	inside
26	Loboc Watershed	150	23,594	20.4	4.967	683	2,017,384	mini	very low	0.0	0.0	0.0	inside
27	Other	156	3787	23.2	0.587	92	272,066	micro	very low	7.8	88.8	−81.0	outside
28	Other	161	192	27.8	0.028	5	15,705	micro	high	7.8	5.1	2.7	outside
29	Loboc Watershed	167	304	29.0	0.049	10	28,505	micro	medium	4.3	9.3	−5.0	outside
30	Loboc Watershed	173	25,689	20.0	5.328	721	2,130,974	mini	medium	0.0	0.0	0.0	inside
31	Wahig-Inabanga Watershed	177	209	29.1	0.050	10	29,027	micro	high	6.3	9.5	−3.2	outside
32	Other	195	2147	25.0	0.344	58	171,157	micro	medium	7.5	55.9	−48.4	outside
33	Other	196	240	33.0	0.039	9	25,362	micro	very high	4.9	8.3	−3.3	outside
34	Other	201	841	21.9	0.124	18	54,179	micro	very high	7.5	17.7	−10.2	outside
35	Other	209	767	29.3	0.179	35	104,667	micro	very high	14.4	34.2	−19.7	outside
36	Other	217	11,295	30.3	2.007	411	1,214,055	mini	low	0.0	0.0	0.0	outside
37	Other	225	216	30.3	0.031	6	18,508	micro	very high	4.5	6.0	−1.5	outside
38	Loboc Watershed	233	25,872	20.5	5.356	740	2,186,165	mini	medium	0.0	0.0	0.0	inside
39	Other	234	267	21.0	0.064	9	26,711	micro	high	5.1	8.7	−3.6	outside
40	Other	238	175	20.0	0.036	5	14,370	pico	high	11.1	4.7	6.4	outside
41	Loboc Watershed	246	46,279	32.7	9.210	2031	6,001,996	small	low	0.0	0.0	0.0	inside
42	Other	249	631	21.4	0.147	21	62,926	micro	very high	19.3	20.5	−1.3	outside
43	Loboc Watershed	251	46,342	21.2	9.220	1322	3,905,939	small	low	0.0	0.0	0.0	inside
44	Other	271	181	32.7	0.037	8	23,857	micro	high	9.3	7.8	1.5	outside
45	Other	284	128	34.3	0.028	7	19,427	micro	very high	11.0	6.3	4.6	outside
46	Loboc Watershed	300	741	29.1	0.150	29	87,155	micro	very high	3.3	28.5	−25.2	inside

Table A1. *Cont.*

Count	Watershed	Catchment ID	Area, ha	Gross Head, m	Flow, m³/s	Power, kW	Annual Energy, kWh	Type	k_{sn} Class	HH_{200m}	HH_{site}	HH_{diff}	Protected Area
47	Other	315	436	25.7	0.103	18	52,956	micro	high	9.3	17.3	−8.0	outside
48	Loboc Watershed	319	47,491	21.1	9.407	1341	3,962,478	small	high	0.0	0.0	0.0	outside
49	Wahig-Inabanga Watershed	333	394	52.7	0.091	32	95,171	micro	very high	9.6	31.1	−21.5	outside
50	Other	346	718	25.2	0.090	15	45,323	micro	very high	9.2	14.8	−5.6	outside
51	Other	348	4231	20.3	0.677	93	273,575	micro	very low	9.3	89.3	−80.0	outside
52	Loboc Watershed	357	1399	50.6	0.250	86	252,673	micro	very high	5.6	82.5	−76.9	outside
53	Other	364	182	27.4	0.043	8	23,702	micro	high	7.5	7.7	−0.3	outside
54	Loboc Watershed	365	49,226	27.3	9.709	1790	5,288,296	small	medium	0.0	0.0	0.0	outside
55	Wahig-Inabanga Watershed	380	105	27.2	0.021	4	11,416	pico	high	4.7	3.7	1.0	outside
56	Wahig-Inabanga Watershed	403	517	36.4	0.110	27	79,789	micro	very high	7.0	26.1	−19.0	inside
57	Wahig-Inabanga Watershed	409	177	20.3	0.039	5	15,693	micro	high	6.2	5.1	1.0	inside
58	Loboc Watershed	418	214	22.3	0.039	6	17,460	micro	medium	2.6	5.7	−3.1	inside
59	Wahig-Inabanga Watershed	430	508	29.0	0.109	21	63,166	micro	very high	5.8	20.6	−14.9	inside
60	Wahig-Inabanga Watershed	446	142	50.3	0.032	11	31,997	micro	very high	3.7	10.4	−6.8	inside
61	Wahig-Inabanga Watershed	457	138	23.9	0.030	5	14,222	pico	high	2.3	4.6	−2.4	outside
62	Other	462	231	28.2	0.049	9	27,272	micro	very high	14.9	8.9	6.0	outside
63	Wahig-Inabanga Watershed	468	384	20.1	0.080	11	31,940	micro	high	3.5	10.4	−7.0	outside
64	Loboc Watershed	471	118	25.5	0.018	3	8996	pico	high	8.1	2.9	5.2	outside
65	Other	475	180	26.0	0.043	8	22,328	micro	high	8.6	7.3	1.3	outside
66	Other	480	130	22.7	0.032	5	14,689	pico	high	9.2	4.8	4.4	inside
67	Loboc Watershed	482	425	22.0	0.081	12	35,507	micro	high	5.9	11.6	−5.7	inside
68	Other	483	330	21.2	0.080	11	33,869	micro	very high	6.8	11.1	−4.3	inside
69	Loboc Watershed	489	237	25.7	0.045	8	22,968	micro	high	3.3	7.5	−4.2	inside
70	Other	492	133	21.4	0.031	5	13,332	pico	high	13.0	4.4	8.6	inside
71	Loboc Watershed	493	306	20.3	0.060	8	24,216	micro	high	6.0	7.9	−1.9	inside
72	Other	497	161	36.3	0.035	9	25,632	micro	very high	5.7	8.4	−2.6	inside
73	Other	510	212	20.1	0.049	7	19,777	micro	high	10.9	6.5	4.5	inside
74	Loboc Watershed	517	274	26.3	0.055	10	29,070	micro	very high	4.1	9.5	−5.4	inside
75	Other	522	134	20.0	0.030	4	11,794	pico	high	5.0	3.9	1.1	outside
76	Other	527	1931	38.8	0.434	114	335,958	mini	medium	0.0	0.0	0.0	inside
77	Other	530	202	21.6	0.049	7	21,022	micro	high	9.1	6.9	2.3	inside
78	Loboc Watershed	536	765	26.1	0.146	26	76,253	micro	very high	4.7	24.9	−20.2	inside
79	Loboc Watershed	546	148	20.3	0.033	5	13,350	pico	high	5.9	4.4	1.5	inside
80	Loboc Watershed	549	141	35.2	0.030	7	20,722	micro	high	39.6	6.8	32.9	inside
81	Other	557	2201	26.2	0.494	87	258,118	micro	low	12.8	84.3	−71.4	inside
82	Other	562	130	27.7	0.031	6	17,264	micro	high	7.9	5.6	2.3	inside
83	Other	567	143	25.0	0.034	6	16,776	micro	very high	8.9	5.5	3.4	inside
84	Other	576	138	33.1	0.027	6	17,661	micro	high	6.0	5.8	0.3	outside
85	Other	582	502	24.2	0.097	16	46,588	micro	very high	4.7	15.2	−10.5	outside
86	Other	588	293	21.9	0.055	8	24,201	micro	high	5.8	7.9	−2.1	outside
87	Other	589	958	20.9	0.186	26	77,659	micro	very high	4.2	25.4	−21.2	outside
88	Loboc Watershed	592	146	21.9	0.026	4	11,349	pico	high	7.9	3.7	4.2	outside
89	Loboc Watershed	595	196	22.2	0.041	6	18,114	micro	medium	6.6	5.9	0.7	outside
90	Other	598	555	23.8	0.128	21	60,815	micro	very high	8.8	19.9	−11.1	outside
91	Loboc Watershed	602	237	33.5	0.043	10	28,374	micro	high	25.8	9.3	16.5	outside
92	Other	608	245	23.5	0.042	7	19,643	micro	very high	7.8	6.4	1.4	outside
93	Other	616	106	22.3	0.020	3	9042	pico	high	13.2	3.0	10.3	outside
94	Other	618	277	20.3	0.049	7	19,875	micro	high	17.8	6.5	11.3	outside

References

1. Avtar, R.; Sahu, N.; Aggarwal, A.K.; Chakraborty, S.; Kharrazi, A.; Yunus, A.P.; Dou, J.; Kurniawan, T.A. Exploring Renewable Energy Resources Using Remote Sensing and GIS—A Review. *Resources* **2019**, *8*, 149. [CrossRef]
2. Hoes, O.A.C.; Meijer, L.J.J.; van der Ent, R.J.; van De, N.C. Systematic high-resolution assessment of global hydropower potential. *PLoS ONE* **2017**, *12*, e0171844. [CrossRef]
3. JICA. Guideline and Manual for Hydropower Development Vol 2 Small Scale Hydropower. 2011. Available online: https://openjicareport.jica.go.jp/pdf/12024899.pdf (accessed on 3 July 2020).
4. Province of Bohol. Bohol Island Power Development Plan (BIPDP). 2017. Available online: http://www.ppdobohol.lgu.ph/plan-reports/development-plans/bohol-island-power-development-plan-bipdp/ (accessed on 21 May 2020).
5. Yi, C.S.; Lee, J.H.; Shim, M.P. Site location analysis for small hydropower using geo-spatial information system. *Renew. Energy* **2010**, *35*, 852–861. [CrossRef]
6. Zhang, J.; Xu, L.; Li, X. Review on the externalities of hydropower: A comparison between large and small hydropower projects in Tibet based on the CO_2 equivalent. *Renew. Sustain. Energy Rev.* **2015**, *50*, 176–185. [CrossRef]
7. IRENA. Renewables Readiness Assessment: The Philippines. *Int. Renew. Energy Agency* **2017**, *10*, 79–89. Available online: https://www.irena.org/publications/2017/Mar/Renewables-Readiness-Assessment-The-Philippines (accessed on 20 June 2021).
8. Faruqui, N.I. Small hydro for rural development. *Can. Water Resour. J.* **1994**, *19*, 227–235. [CrossRef]
9. Mayor, B.; Rodríguez-Muñoz, I.; Villarroya, F.; Montero, E.; López-Gunn, E. The role of large and small scale hydropower for energy and water security in the Spanish Duero basin. *Sustainability* **2017**, *9*, 1807. [CrossRef]
10. Asian Development Bank. The Philippines: Energy Sector Assessment, Strategy, and Road Map. 2016. Available online: https://www.adb.org/sites/default/files/institutional-document/218286/mya-energy-sector-assessment.pdf (accessed on 5 May 2020).
11. Philippine Department of Energy. Renewable Energy Decade Report 2008–2018. 2019. Available online: https://www.doe.gov.ph/renewable-energy/empowered-renewable-energy-decade-report-2008-2018?ckattempt=1 (accessed on 12 January 2021).
12. Fasipe, O.A.; Izinyon, O.C.; Ehiorobo, J.O. Hydropower potential assessment using spatial technology and hydrological modelling in Nigeria river basin. *Renew. Energy* **2021**, *178*, 960–976. [CrossRef]
13. Moiz, A.; Kawasaki, A.; Koike, T.; Shrestha, M. A systematic decision support tool for robust hydropower site selection in poorly gauged basins. *Appl. Energy* **2018**, *224*, 309–321. [CrossRef]
14. Thin, K.K.; Zin, W.W.; San, Z.M.L.T.; Kawasaki, A.; Moiz, A.; Bhagabati, S.S. Estimation of run-of-river hydropower potential in the myitnge river basin. *J. Disaster Res.* **2020**, *15*, 267–276. [CrossRef]
15. Bayazıt, Y.; Bakış, R.; Koç, C. An investigation of small scale hydropower plants using the geographic information system. *Renew. Sustain. Energy Rev.* **2017**, *67*, 289–294. [CrossRef]
16. Sammartano, V.; Liuzzo, L.; Freni, G. Identification of potential locations for run-of-river hydropower plants using a GIS-based procedure. *Energies* **2019**, *12*, 3446. [CrossRef]
17. Tarife, R.P.; Tahud, A.P.; Gulben, E.J.G.; Macalisang, H.A.R.C.P.; Ignacio, M.T.T. Application of geographic information system (GIS) in hydropower resource assessment: A case study in Misamis Occidental, Philippines. *Int. J. Environ. Sci. Dev.* **2017**, *8*, 507–511. [CrossRef]
18. Guiamel, I.A.; Lee, H.S. Potential hydropower estimation for the Mindanao River Basin in the Philippines based on watershed modelling using the soil and water assessment tool. *Energy Rep.* **2020**, *6*, 1010–1028. [CrossRef]
19. Jafari, M.; Fazloula, R.; Effati, M.; Jamali, A. Providing a GIS-based framework for Run-Of-River hydropower site selection: A model based on sustainable development energy approach. *Civ. Eng. Environ. Syst.* **2021**, *38*, 102–126. [CrossRef]
20. Tamm, O.; Tamm, T. Verification of a robust method for sizing and siting the small hydropower run-of-river plant potential by using GIS. *Renew. Energy* **2020**, *155*, 153–159. [CrossRef]
21. Marston, R.A.; Butler, W.D.; Patch, N.L. Geomorphic Hazards. In *International Encyclopedia of Geography: People, the Earth, Environment and Technology*; John Wiley & Sons, Inc.: Hoboken, NJ, USA, 2017.
22. Schwanghart, W.; Ryan, M.; Korup, O. Topographic and seismic constraints on the vulnerability of Himalayan hydropower. *Geophys. Res. Lett.* **2018**, *45*, 8985–8992. [CrossRef]
23. Geach, M.R.; Stokes, M.; Hart, A. The application of geomorphic indices in terrain analysis for ground engineering practice. *Eng. Geol.* **2017**, *217*, 122–140. [CrossRef]
24. Mudd, S.M.; Clubb, F.J.; Gailleton, B.; Hurst, M.D. How concave are river channels? *Earth Surf. Dyn.* **2018**, *6*, 505–523. [CrossRef]
25. Whipple, K.X.; Tucker, G.E. Dynamics of the stream-power river incision model: Implications for height limits of mountain ranges, landscape response timescales, and research needs. *J. Geophys. Res.* **1999**, *104*, 661–674. [CrossRef]
26. Boulton, S.J. Geomorphic response to differential uplift: River long profiles and knickpoints from Guadalcanal and Makira (Solomon Islands). *Front. Earth Sci.* **2020**, *8*, 1–23. [CrossRef]
27. Castillo, M.; Muñoz-Salinas, E.; Ferrari, L. Response of a landscape to tectonics using channel steepness indices (ksn) and OSL: A case of study from the Jalisco Block, Western Mexico. *Geomorphology* **2014**, *221*, 204–214. [CrossRef]
28. Schwanghart, W.; Scherler, D. Short Communication: TopoToolbox 2-MATLAB-based software for topographic analysis and modeling in Earth surface sciences. *Earth Surf. Dyn.* **2014**, *2*, 1–7. [CrossRef]
29. Chen, Y.W.; Shyu, J.B.H.; Chang, C.P. Neotectonic characteristics along the eastern flank of the Central Range in the active Taiwan orogen inferred from fluvial channel morphology. *Tectonics* **2015**, *34*, 2249–2270. [CrossRef]

30. Ross, C.W.; Prihodko, J.Y.L.; Anchang, S.S.K.; Ji, W.; Hanan, N.P. Global Hydrologic Soil Groups (HYSOGs250m) for Curve Number-Based Runoff Modeling. *Sci. Data* **2018**, *5*, 180091. [CrossRef] [PubMed]

31. Buchhorn, M.; Smets, B.; Bertels, L.; De Roo, B.; Lesiv, M.; Tsendbazar, N.E.; Li, L.; Tarko, A.J. *Copernicus Global Land Service: Land Cover 100m: Version 3 Globe 2015–2019: Product User Manual*; Zenodo: Geneve, Switzerland, September 2020; pp. 1–93. [CrossRef]

32. Fick, S.E.; Hijmans, R.J. WorldClim 2: New 1-km spatial resolution climate surfaces for global land areas. *Int. J. Climatol.* **2017**, *37*, 4302–4315. [CrossRef]

33. Pojadas, D.J.; Abundo, M.L.S. Spatio-temporal assessment and economic analysis of a grid-connected island province toward a 35% or greater domestic renewable energy portfolio: A case in Bohol, Philippines. *Int. J. Energy Environ. Eng.* **2021**, *12*, 251–280. [CrossRef]

34. Bergström, D.; Malmros, C. Finding Potential Sites for Small-Scale Hydro Power in Uganda: A Step to Assist the Rural Electrification by the Use of GIS. Geobiosphere Science Centre, Department 2005, 95. Available online: http://www.natgeo.lu.se/ex-jobb/exj_121.pdf (accessed on 14 April 2020).

35. Arthur, E.; Anyemedu, F.O.K.; Gyamfi, C.; Tannor, P.A.; Adjei, K.A.; Anornu, G.K.; Odai, S.N. Potential for small hydropower development in the Lower Pra River Basin, Ghana. *J. Hydrol. Reg. Stud.* **2020**, *32*, 100757. [CrossRef]

36. Sekac, T.; Jana, S.K.; Pal, D.K. Identifying potential sites for hydropower plant development in Busu catchment: Papua New Guinea. *Spat. Inf. Res.* **2017**, *25*, 791–800. [CrossRef]

37. Tian, Y.; Zhang, F.; Yuan, Z.; Che, Z.; Zafetti, N. Assessment power generation potential of small hydropower plants using GIS software. *Energy Rep.* **2020**, *6*, 1393–1404. [CrossRef]

38. Hashim, H.Q.; Sayl, K.N. Detection of suitable sites for rainwater harvesting planning in an arid region using geographic information system. *Appl. Geomat.* **2020**, *13*, 235–248. [CrossRef]

39. USDA-NRCS. Part 630 Hydrology National Engineering Handbook Chapter 7 Hydrologic Soil Groups. In *National Engineering Handbook*; Natural Resources Conservation Services—United States Department of Agriculture: Washington DC, USA, 2009.

40. NWRB-DENR. Resolution No. 03 0613. Revised Policy on Granting Water Rights over Surface Water or Hydropwer Projects. 2013. Available online: http://www.nwrb.gov.ph/images/Board_Resolution/Res_03-0613.pdf (accessed on 14 May 2021).

41. Singh, D. *Micro Hydro Power Resource Assessment Handbook*; Asian and Pacific Centre for Transfer of Technology of the United Nations—Economic and Social Commission for Asia and the Pacific (ESCAP): New Delhi, India, 2009; p. 69.

42. Mdee, O.J.; Kimambo, C.Z.; Nielsen, T.K.; Kihedu, J. Measurement methods for hydropower resources: A review. *Water Util. J.* **2018**, *18*, 21–38.

43. Wobus, C.; Whipple, K.X.; Kirby, E.; Snyder, N.; Johnson, J.; Spyropolou, K.; Crosby, B.; Sheehan, D. Tectonics from topography: Procedures, promise, and pitfalls. *Tecton. Clim. Landsc. E* **2006**, *398*, 55–74. [CrossRef]

44. Kothyari, G.C.; Kotlia, B.S.; Talukdar, R.; Pant, C.C.; Joshi, M. Evidences of neotectonic activity along Goriganga River, Higher Central Kumaun Himalaya, India. *Geol. J.* **2020**, *55*, 6123–6146. [CrossRef]

45. Lague, D. The stream power river incision model: Evidence, theory and beyond. *Earth Surf. Process. Landf.* **2014**, *39*, 38–61. [CrossRef]

46. Willett, S.D.; McCoy, S.W.; Perron, J.T.; Goren, L.; Chen, C.Y. Dynamic reorganization of River Basins. *Science* **2014**, *343*, 1–19. [CrossRef]

47. Harel, M.A.; Mudd, S.M.; Attal, M. Global analysis of the stream power law parameters based on worldwide 10Be denudation rates. *Geomorphology* **2016**, *268*, 184–196. [CrossRef]

48. Kirby, E.; Whipple, K.X. Expression of active tectonics in erosional landscapes. *J. Struct. Geol.* **2012**, *44*, 54–75. [CrossRef]

49. UNEP-WCMC. *User Manual for the World Database on Protected Areas and World Database on Other Effective Area-Based Conservation Measures: 1.6*; NEP-WCMC: Cambridge, UK, 2019. Available online: http://wcmc.io/WDPA_manual (accessed on 4 April 2020).

50. *RA No. 11038. Expanded National Integrated Protected Areas Sytem (NIPAS) Act of 2018*; Congress of the Philippines: Manila, Philippines, 2018.

51. Philippine Statistics Authority. Highlights on Household Population, Number of Households, and Average Household Size of the Philippines (2015 Census of Population). 2016. Available online: https://psa.gov.ph/content/highlights-household-population-number-households-and-average-household-size-philippines#:~{}:text=Thecountry\T1\textquoterightsaveragehouseholdsize,to4.4personsin2015 (accessed on 8 June 2021).

52. Philippine Department of Energy. *List of Existing Power Plants (Grid-Connected) As of June 2019 Department of Energy List of Existing Power Plants (Grid-Connected) As of June 2019*; Philippine Department of Energy: Manila, Philippines, 2019.

53. Carrasco, J.L.; Pain, A.; Spuhler, D. Hydropower (Small-Scale). Sustainable Sanitation and Water Management Toolbox-SSWM.info. 2019. Available online: https://sswm.info/water-nutrient-cycle/water-distribution/hardwares/water-network-distribution/hydropower-%28small-scale%29 (accessed on 2 June 2020).

54. Tucker, G.E.; Hancock, G.R. Modelling landscape evolution. *Earth Surf. Process. Landf.* **2010**, *35*, 28–50. [CrossRef]

55. Ugwu, C.O.; Ozor, P.A.; Mbohwa, C. Small hydropower as a source of clean and local energy in Nigeria: Prospects and challenges. *Fuel Commun.* **2022**, *10*, 100046. [CrossRef]

56. Garegnani, G.; Sacchelli, S.; Balest, J.; Zambelli, P. GIS-based approach for assessing the energy potential and the financial feasibility of run-off-river hydro-power in Alpine valleys. *Appl. Energy* **2018**, *216*, 709–723. [CrossRef]

57. Magaju, D.; Cattapan, A.; Franca, M. Identification of run-of-river hydropower investments in data scarce regions using global data. *Energy Sustain. Dev.* **2020**, *58*, 30–41. [CrossRef]

58. Cai, X.; Ye, F.; Gholinia, F. Application of artificial neural network and Soil and Water Assessment Tools in evaluating power generation of small hydropower stations. *Energy Rep.* **2020**, *6*, 2106–2118. [CrossRef]

59. Department of Environment and Natural Resources. *Implementing Rules and Regulations of Republic Act 7586 or the National Integrated Protected Areas System (NIPAS) Act of 1992, as Amended by Republic Act 11038 or the Expanded National Protected Areas System (ENIPAS) Act of 2018*; DENR: Quezon City, Philippines, 2019. Available online: https://www.officialgazette.gov.ph/downloads (accessed on 21 October 2021).

60. Manzano-Agugliaro, F.; Taher, M.; Zapata-Sierra, A.; Juaidi, A.; Montoya, F.G. An overview of research and energy evolution for small hydropower in Europe. *Renew. Sustain. Energy Rev.* **2017**, *75*, 476–489. [CrossRef]